Hydrologic-Hydraulic Model for Simulating Dual Drainage and Flooding in Urban Areas: Application to a Catchment in the Metropolitan Area of Chicago

Citation	Nanía, L. S., León, A. S., & García, M. H. (2015). Hydrologic-Hydraulic Model for Simulating Dual Drainage and Flooding in Urban Areas: Application to a Catchment in the Metropolitan Area of Chicago. Journal of Hydrologic Engineering, 20(5), 04014071. doi:10.1061/(ASCE)HE.1943-5584.0001080
DOI	10.1061/(ASCE)HE.1943-5584.0001080
Publisher	American Society of Civil Engineers
Version	Accepted Manuscript
Terms of Use	http://cdss.library.oregonstate.edu/sa-termsofuse

A HYDROLOGIC-HYDRAULIC MODEL FOR SIMULATING DUAL DRAINAGE AND FLOODING IN URBAN AREAS: APPLICATION TO A CATCHMENT IN THE METROPOLITAN AREA OF CHICAGO, IL

Leonardo S. Nanía[1], Arturo S. León[2] Marcelo H. García[3]
[1] Associate Professor, Dept. of Structural Mechanics and Hydraulic Engineering, Universidad de Granada, Campus de Fuentenueva, Granada 18071, SPAIN. E-mail: LNania@ugr.es
[2] P.E., D.WRE, M.ASCE, Assistant Professor, School of Civil and Construction Engineering, Oregon State University, 220 Owen Hall, Corvallis, OR 97331-3212, USA. E-mail: arturo.leon@oregonstate.edu
[3] Dist.M.ASCE, F.EWRI, Professor and Director, Ven Te Chow Hydrosystems Lab., Dept. of Civil and Envir. Eng., University of Illinois, Urbana, IL 61801, USA. E-mail: mhgarcia@illinois.edu

Abstract

A 1D hydrologic-hydraulic model for simulating dual drainage in urban areas is presented. It consists of four modules: (1) rainfall-runoff transformation, (2) one-dimensional (1-D) flow routing on a street network, (3) flow interception at street inlets and (4) flow interaction between surface water on the streets and the underground storm-water system by interfacing with the EPA-SWMM5 engine (Environmental Protection Agency-Storm Water Management Model). The hydrologic model (first module) transforms rainfall to runoff using the kinematic wave approximation and simulates the infiltration process with the Green-Ampt method. The street network model (second module) is based on a finite-volume shock-capturing scheme that solves the fully conservative Saint-Venant equations and can be used to model both subcritical and supercritical flows. The inlet model (third module) uses the HEC-22 relations to compute the amount of water intercepted by inlets. The formulation of boundary conditions at the street crossings is generalized and can be used for any number of streets, any combination of inflowing and outflowing streets, and flow regime (e.g., subcritical and supercritical flows). Flow interaction between surface water on the streets and underground storm-water system is achieved by interfacing the proposed model with EPA-SWMM5. This interaction allows flow to enter

from streets to the underground storm-water system and vice versa. The proposed model has several potential applications such as the identification of critical zones for flooding (e.g., zones with high water depths and flow velocities) in urban developments and can be used to take appropriate measures for drainage control (e.g., to increase number and/or size of inlets), to determine the consequences of different degrees of inlet clogging, and to assess flooding hazards through the application of suitable hazard criteria. A summary of criteria used for storm-water hazard assessment is presented. To demonstrate the dual-drainage model's potential an application is performed in a catchment of the metropolitan area of Chicago, IL. The results obtained are promising and show that the model can be a useful tool for storm water management and flooding hazard assessment in urban areas.

Introduction

Urban catchments in rainy climates are commonly exposed to flood threats. In lowland areas urban flooding is often associated with an inadequate drainage system, in most cases due to inadequate inlet capacity. Urban flooding may cause material losses in the form of public and private property damage and even human casualties. Furthermore, street flooding may interfere with traffic and in some cases, may jeopardize pedestrian safety. To identify critical urban flooding areas (e.g., zones with high water depths and/or flow velocities) so that appropriate measures for flow control and drainage (e.g., to add inlet grates) can be taken, hydrologic and hydraulic (H&H) modeling is often required. In many instances H&H modeling could involve large urban catchments making it necessary to increase computational efficiency without sacrificing accuracy. For a flood modeling tool to be practical, the flooding analysis needs to be

done in a relatively short time frame so that flash flood warnings can be issued and traffic redirected to reduce emergencies and facilitate the work of first responders..

A number of researchers have addressed the problem of modeling pluvial flows in urban areas. Although the idea of studying flows in urban areas involving surface (overland) and subsurface (pipe) components and their interaction has been around for several decades, Djordjevic et al (1999) first advanced it, using the BEMUS model for surface flows and a sewer model that allowed for computing pressurized flows. The interaction consisted in the connection between manholes and computational cells in the surface. At about the same time, Hsu et al (2000) used the SWMM model to simulate pipe flow and, when pressurized, to generate the flows that a 2D-non-inertia model conveyed over the surface. A drawback of this approach is that the flow is not allowed to re-enter the sewer system. Schmitt et al (2004) studied flooding in urban drainage systems by a combination of 2D model for surface flow and 1D model for pipe flow in which manholes were connected to 2D elements. A year later, Djordjevic et al (2005) presented a 1D/1D model (SIPSON) to simulate dual drainage in two parallel networks (streets and pipes) linked through nodes representing a group of inlets. In this work, the hydrological component was not described in much detail, and inflows to and from nodes were computed with the help of weir and orifice formulas. The possibility of a manhole lid to be removed was also taken into account. Aronica and Lanza (2005) simulated urban flows by using a 2D model addressing only surface flows and analyzed the effect of including or not the inlets (i.e. sewer system with assumed unlimited conveyance capacity or with no sewer system). No explanation was given for computing inlet capacity. Kumar et al (2007) combined the EXTRAN module of SWMM and another 1D module for river flows with a 2D model for surface flow, linking them with an interface using weir formulas. More recently, Chen et al (2010) studied the combined

76 consequences of pluvial and fluvial flooding combining the SIPSON model (Djordjevic et al,
77 2005) for pluvial flooding and 2D, non-inertia UIM model for fluvial flooding. The latest
78 research work has been devoted to the numerical and experimental study of the flow interaction
79 between the street and the underground sewer system (Bazin et al, 2013 and Djordjevic et al.,
80 2013) as well as the hydraulic characterization of storm water inlets (Martins et al, 2014).
81 The model presented herein has characteristics similar to the one presented by Djordjevic et al
82 (2005) since a street network conveys surface flows and interaction is allowed with underground
83 storm-water network. From a modeling standpoint, the main contributions of this work are as
84 follows:
85 1) Rainfall-runoff transformation (hydrological module) is simulated by computing overland
86 flow in two parallel planes, including infiltration process. Subcatchments are composed by the
87 portions of blocks that pour to the adjacent street (Nanía, 1999 and Nanía et al, 2004). The
88 representation of subcatchments is made simple to facilitate its implementation in large urban
89 areas.
90 2) Runoff generated in the subcatchments (item 1) is incorporated uniformly distributed and
91 routed through the streets. A 1D formulation is used to route the flow on the street network.
92 3) Flow distribution in four-branch crossings of the street network involving both supercritical
93 and subcritical flows is computed using empirical relationships presented by Nanía et al (2004,
94 2011) when applicable. The formulation of boundary conditions at the street crossings is
95 generalized and can be used for any number of streets, any combination of inflowing and
96 outflowing streets and any flow regime.
97 4) Inlet flows at streets are simulated using the HEC-22 formulation (FHA, 2001).

5) Flow interaction between surface water on the streets and the underground storm-water sewers is simulated by interfacing the street network model with the EPA-SWMM5 engine.

In order to illustrate the capabilities of the model, it was applied to a catchment in Dolton, a southern suburb of the metropolitan area of Chicago. The watershed considered in this analysis drains to drop-shaft CDS-51 in the Calumet TARP (Tunnel and Reservoir Plan) system which is managed by the Metropolitan Water Reclamation District of Greater Chicago (MWRDGC). The topography of the zone is quite flat and mainly subcritical flows are expected to take place most of the time.

Model description

This work aims at developing an integrated model to simulate the hydrology and hydraulics of urban drainage systems. This integrated model has four modules. The first module is a hydrologic model, which transforms rainfall into effective runoff depending on surface characteristics (e.g., slope, roughness, paved/unpaved surface area). The resulting runoff from each block is distributed over the respective street and is used as input for the hydraulic street model (second module). The street module routes the flow over the street network. The third module estimates flow interception at inlets, which conveys street runoff into the underground storm-sewer system. The intercepted runoff is used as input for the storm-sewer model which is modeled using the EPA-SWMM5 engine. A brief overview of these modules is presented next.

<u>First module: hydrologic model</u>

The hydrologic model transforms rainfall to runoff considering both impervious and pervious surfaces and simulates the infiltration process with the Green-Ampt method (Chow et al, 1988). The depression storage (initial abstraction) is also considered in order to obtain the effective

rainfall. The transformation from effective rainfall to runoff is made considering overland flow on two independent equal-length sloping planes, one pervious and one impervious, and using the kinematic wave approximation of the Saint Venant equations (Chow et al, 1988). The subcatchments are delineated as part of the blocks which are computed simply based on polygons defined by the surrounding streets, which in turn are determined by the position of the street junctions (crossings). Runoff is introduced uniformly distributed in the streets surrounding the blocks, therefore impervious and pervious areas are not directly connected to the sewer system.

Second module: street flow routing

The street module solves the one-dimensional open-channel flow continuity and momentum equations that for non-prismatic channels or rivers may be written in vectorial conservative form as follows (e.g., Chaudhry 1987, Leon 2007, Leon et al. 2006, 2010a):

$$\frac{\partial \mathbf{U}}{\partial t} + \frac{\partial \mathbf{F}}{\partial x} = \mathbf{S} \tag{1}$$

where the vector variable **U**, the flux vector **F** and the source term vector **S** are given respectively by:

$$\mathbf{U} = \begin{bmatrix} A \\ Q \end{bmatrix}; \mathbf{F} = \begin{bmatrix} Q \\ \frac{Q^2}{A} + \frac{A\overline{p}}{\rho} \end{bmatrix}; \mathbf{S} = \begin{bmatrix} 0 \\ F_w + \left(S_0 - S_f\right) gA \end{bmatrix} \tag{2}$$

where A = cross-sectional area of the channel; Q = flow discharge; $\overline{p}$ = average pressure of the water column over the cross sectional area; ρ = water density; g = gravitational acceleration; S_o = slope of the channel bottom; S_f = energy slope , which may be estimated using an empirical formula such as Manning's equation; and F_w = momentum term arising from the longitudinal variation of the channel width.

142 The governing equations (1)-(2) are solved using a Finite Volume (FV) shock-capturing scheme
143 in an identical way to that presented in León et al. (2006, 2010a, 2013). The FV scheme used is
144 the second-order MUSCL-Hancock method with the MINMOD Total Variation Diminishing
145 (TVD) pre-processing slope limiter. The FV-shock capturing scheme used ensures that mass and
146 momentum are conserved. For the boundary conditions at the street crossings an identical
147 approach to that presented in León et al. (2009) and León et al. 2010b) was used. These
148 boundary conditions use the equation of energy, equation of continuity and the theory of
149 Riemann invariants. These boundary conditions can be used for any number of streets, any
150 combination of inflowing and outflowing streets, and any flow regime (e.g., supercritical flow).
151 For more details about these boundary conditions the reader is referred to León et al. (2009,
152 2010b). From a hydraulics point of view, the main interest is in estimating the average velocities
153 and water depths in the area under study. Because of this, it is expected that a one-dimensional
154 unsteady flow model is appropriate for this application.
155 Flow distribution in four-branch crossings of the street network involving both supercritical and
156 subcritical flows is computed using relations presented by Nanía et al (2004, 2011) when
157 applicable. This is a relevant new contribution to urban drainage models.
158 Third module: inlets
159 The third module comprises a model for estimating flow interception at inlets, which leads street
160 runoff into the underground storm-sewer system. The inlet module in the proposed model was
161 implemented according to the HEC-22 manual (Federal Highway Administration, 2001). The
162 HEC-22 manual comprises a wide array of storm drain inlets. Overall, inlets can be divided
163 (Federal Highway Administration, 2001) into (1) Grate inlets, (2) Curb-opening inlets, (3)
164 Slotted inlets, and (4) Combination inlets. Grate inlets consist of an opening in the gutter or ditch

165 covered by a grate. Curb-opening inlets are vertical openings in the curb covered by a top slab.
166 Slotted inlets consist of a pipe cut along the longitudinal axis with bars perpendicular to the
167 opening to maintain the slotted opening. Combination inlets consist of both a curb-opening inlet
168 and a grate inlet placed in a side-by-side configuration, but the curb opening may be located in
169 part upstream of the grate. The inlet module of the current proposed model includes grate inlets,
170 curb opening and combination inlets. The grate types implemented include P-50, P-30 and
171 curved vane. Any other type of inlet and grate type can be readily implemented in the model, if
172 necessary.

173 Fourth module: storm-water system

174 The current version of the street network model so-called Street Flooding Model (SFM) is
175 coupled with the EPA-SWMM5 engine through a coupling interface which manages the flow
176 intercepted by inlets in the following way:

177 1) Intercepted flow by inlets enters in the nodes of the sewer system (manholes). By default,
178 it is assumed that every inlet is connected to the nearest manhole, but it could be
179 configured by the user.
180 2) Flow enters the node only if the node is not flooded, this is, if the hydraulic grade line is
181 lower than the ground elevation.
182 3) If a given node is flooded (hydraulic grade line is either higher or equal the ground
183 elevation) the flooded volume computed by SWMM5 is incorporated to the street
184 network through the inlets connected to the flooded node. The flooded volume is
185 distributed evenly between all the inlets connected to that node and in the time between
186 interface callings.

187 The coupling interface calls the SWMM5 at a pre-defined time step which could be as low as the
188 computing time step (less than one second). However, such small coupling time would increase
189 excessively the computing time because a "sleeping time" of 1 second is allowed after the calling
190 of the EPA-SWMM5 engine in order to allow for writing of some required files. A coupling time
191 of 10 seconds was found to be not too short to penalize computing time and not too long to have
192 a decisive influence on the results. Therefore, in case of flooding, the flooded discharge is
193 updated as often as the coupling time.
194
195 **Criteria used for the surface storm-water hazard assessment**
196 The main objective of an urban drainage system is to safeguard the security of the citizen's
197 activities, which means: avoiding water entering buildings and houses, allowing pedestrians to
198 walk unobstructed and permitting traffic to move safely. In some cases it is also used to avoid
199 pollution in urban areas with combined sewers.
200 In principle, urban runoff should be such that the hydraulic parameters i.e. depths, velocities or
201 some combinations of depth and velocities remain below certain advisable limit values. There is
202 not much research in the literature about safety criteria for the drainage flow in urban zones. The
203 following criteria could potentially be used to assess flood-induced hazards:
204 Criteria based on a maximum admissible depth
205 Concerning material damage and its minimization we can accept as a maximum depth, a flow
206 depth for which urban runoff does not enter commercial and residential buildings.
207 *Denver's criterion:* The Urban Storm Drainage Criteria Manual of Denver, Colorado (Wright-
208 McLaughlin, 1969), establishes that in local streets depending on the category of the streets of
209 the studied sub-basin, a flow depth is allowed so that the free surface of the flow does not

overcome the level of the ground floor of residential, public, commercial and industrial buildings unless they are waterproofed, and a maximum 45.7 cm (18 inches) over the lowest level of the street is permitted. This criterion becomes more restrictive in streets of a higher category. This limit seems to be established based on the minimization of traffic problems, bearing in mind that driving a car in streets with flow depths larger than 45.7 cm would be both dangerous and unsuitable.

Clark County's criterion: The Hydrologic Criteria and Drainage Design Manual of Clark County Regional Flood Control District (CCRFCD, 1999) establishes for minor storms that local streets, narrower than 24 m, can transport water up to a depth of 30 cm, measured along the gutter flow line.

Austin's criterion: In other cities, like Austin, Texas (City of Austin Dept. of Public Works, 1977), the criterion of leaving the crown of the street free in such a way that emergency vehicles (fire trucks, ambulances, police cars) will be able to move along this zone is commonly used. So an implicit maximum depth is defined by establishing a permissible spread of water ranging from 0 (not exceed crown level) to 7.2 m depending on the street type.

Mendoza's criterion: Nanía (1999) proposed a maximum admissible depth of 30 cm (about 12 inches) given the characteristics of the city where it was used (Mendoza, Argentina) and following the city of Denver's criterion.

Criteria based on flow depth and flow velocity as a combination

Témez's criterion: Témez (1992) defines a "dangerous flooding zone" as a zone where a serious danger of human life loss or significant personal injury exists. This zone is defined by a flow depth greater than 1 m, by a flow velocity greater than 1 m/s and by a product of flow depth times flow velocity (i.e. specific flow discharge) greater than 0.5 m^2/s. This criterion was created

233 to be applied to floodplains. A limit depth of 1 m would be excessive in a densely populated
234 zone like the suburbs of Chicago since such a depth, even without taking into account the
235 velocity of flow, would most likely cause substantial material losses. In this criterion, the product
236 of flow depth times the velocity of 0.5 m^2/s would be less restrictive than the product of the
237 maximum depth of both former criteria times the maximum velocity proposed by Témez (i.e.
238 0.30 m^2/s and 0.45 m^2/s, for Mendoza and Denver, respectively).
239 *Abt's criterion:* Témez's criterion of $Vy < 0.5$ m^2/s for flow depths between 0.5 to 1 m was
240 apparently inspired by the experiments carried out by Abt et al. (1989) to identify when an adult
241 human could not stand or maneuver in a simulated flood flow. Flow velocities of 0.36 to 3.05
242 m/s and flow depths of 0.49 to 1.2 m were considered in the experiments. For these flow
243 conditions, Abt et al. (1989) found that the product of flow velocity times depth which resulted
244 in instabilities was 0.70 to 2.12 m^2/s, depending on the height and weight of subjects. According
245 to these values, using a limit of 0.5 m^2/s independently of the height and weight of a given
246 subject, imply considering a factor of safety ranging from 1.4 to 4.2.
247 *Clark County criterion:* The Hydrologic Criteria and Drainage Design Manual of Clark County
248 Regional Flood Control District (1999) established that for minor storms and local streets
249 (narrower than 24 m) that the product of flow depth in the gutter flow line times the average
250 velocity should be less than or equal to 0.55 m^2/s. This value is a little greater than the value
251 taking in Abt's criterion, so we will consider Abt's criterion as a reference.
252 *New South Wales criterion:* The Floodplain Development Manual of the New South Wales
253 Government (2005) in Australia, proposed a starting point for the determination of hazard
254 categories in floodplain zones, indicating that zones with floodwaters which have either depths
255 greater than 1m, velocities greater than 2 m/s or depths greater than [1m – 3/10 s * velocity

256 (m/s)] should be categorized as high hazard zones. In light of this criterion, the limiting depths
257 for Mendoza (0.30 m) and Denver (0.45 m) are achieved with velocities of 2.33 and 1.83 m/s,
258 respectively, therefore the joint consideration of this criterion and the limiting depths would be
259 approximately equivalent to a maximum velocity of 2 m/s.
260 *No slipping criterion:* Nanía (1999) proposed a momentum-based criterion taking into account
261 the stability to slip by a pedestrian in the presence of the urban runoff, which is defined by:

262 $$V^2 y \leq 1.23 \frac{m^3}{s^2} \quad (3)$$

263 *Stability to tilt criterion:* the Hydraulic and Hydrologic Engineering Dept. of Technical
264 University of Catalonia (2001) carried out a study in order to analyze the spacing of gutters in
265 the City of Barcelona. In this study, a hazard criterion taking into account the stability to tilt of a
266 pedestrian (ability to stay upright) in the presence of urban runoff was defined as:

267 $$Vy \leq 0.5 \frac{m^2}{s} \quad (4)$$

268

269 **Evaluation of the model**

270 The primary objective of this section is to illustrate potential applications of the model. Four
271 typical applications could be:

272 1) Identifying critical zones that would need attention when most of the inlets in the urban
273 watershed are clogged with debris. This would require using the first and second module
274 only.
275 2) Analyzing the hydraulic performance of an actual surface drainage system when most of
276 the inlets are well maintained.

3) Determining the optimum surface drainage system (number, type and position of inlets) in order to achieve a safety criteria against surface stormwater hazards. An optimization algorithm would be required.
4) Determining the optimum sizing of a sewer system (e.g., diameter of pipes) for a given inlet system. This would also require an optimization algorithm.

The model was applied to an urban catchment in the Village of Dolton, a southern suburb of the metropolitan area of Chicago. This watershed was previously used for hydrologic and hydraulic studies of the Tunnel and Reservoir Plan (TARP) conducted by the Ven Te Chow Hydrosystems Laboratory, University of Illinois (Cantone and Schmidt, 2011).

Project storm

In the current application the triangular storm hyetograph proposed by Chow and Yen was used (Chow and Yen, 1976). The storm which is depicted in Figure 1 has a duration of 80 minutes and a maximum intensity of 45.72 mm/h at 30 minutes and it is a simplification of the storm that occurred in Chicago on July 2nd, 1960.

Characteristics of the CDS-51 watershed

CDS-51 is the name given to the dropshaft that captures the pluvial waters from the sewer system of the suburb of Dolton. The main characteristics of the CDS-51 watershed are presented in Table 1.

The street network which is depicted in Figure 2 is composed by 267 blocks (or fraction of blocks), 454 nodes (street crossings) and 637 streets, being the total area modeled of 3.549 km^2 (approx. 2.22 sq. miles). Due to lack of more detailed data, the characteristics of the entire watershed were assigned to every block. Similarly, the cross-section depicted in Figure 3 was assigned to every street. It is worth mentioning that every block can have their own

300 characteristics and every street a different cross-section but keeping the same order of every part
301 (sidewalk, curb, gutter, street, gutter, curb, sidewalk).
302 The street network was defined using DEM data with a resolution of 0.91x0.91m (3x3 feet) with
303 the following procedure: (1) For a given aerial photograph or a shape file of a previously
304 digitalized street network the geo-referenced coordinates x, y and z of every junction (node) are
305 extracted; (2) by combining these coordinates and the morphology of the network (i.e. links
306 between streets and nodes; and links between blocks and nodes), the street lengths, street slopes,
307 angles between streets, area of blocks, and other necessary parameters are computed. The
308 Manning coefficients can vary from street to street, however in this application a value of 0.015
309 was adopted for all streets and sidewalks, which corresponds to concrete. In the whole street
310 network only 120 nodes (street crossings) have four branches. Flow distribution in a particular
311 type of street crossing (four-branch, two inflows forming a right angle) is computed using
312 empirical relationships developed by Nanía et al (2004, 2011). In this case, the number of such
313 crossings varies in time from 25 to 50 because of the alternating flow direction in some streets.
314 Inlet Characteristics
315 Three scenarios with inlets were considered:
316 1) One pair of inlet is considered in every street which is located at 90% of the street length
317 in the direction of the longitudinal bed slope (Scenario 1b).
318 2) Two pairs of inlets are considered in every street and are located at 50% and 90% of the
319 street length in the direction of the longitudinal bed slope (Scenario 1c).
320 3) The actual number and position of inlets is considered (Scenario 2).

In all cases the transversal slope of the gutter was 8%, grate type P-30 according to HEC-22 (FHA, 2001), grate size of 0.60m of width by 0.30m of length, with no curb opening and no depression (type I according to HEC-22 classification).

Characteristics of the sewer system

The sewer system is presented in Figure 4 and it consists of 723 nodes and 722 conduits. In the case of actual inlets, 823 inlets were considered which are connected to 324 nodes. Manning coefficient adopted for concrete sewer conduits was 0.015. They could also vary from conduit to conduit accordingly.

Results

In this section, the results of four different scenarios are presented to demonstrate the potential of the model. The simulated scenarios were:

1) Not considering sewer system:
    a. No inlets (only first and second module). This scenario could be used to find critical areas in the case that 100% of inlets are clogged.
    b. One pair of inlets per street: (first, second and third module) no interaction between surface and sewer system is considered. This scenario and the next one could be used to design the number, position and type of inlets, assuming a large sewer system that never gets flooded. The pair of inlets is located at 90% of the length of the street in the direction of the street slope.
    c. Two pairs of inlets per street: (first, second and third module) no interaction between superficial and sewer system is considered. One pair of inlets is located

343 at 50% the other at 90% of the length of the street in the direction of the street
344 slope.
345 2) Considering sewer system (four modules, dual drainage): with actual inlet number and
346 position but assuming equal grate type due to lack of such data. Interaction with sewer
347 system every 10 seconds is considered.
348 Scenarios 1x)
349 In Figure 5 a summary of the results of the simulations for scenarios 1a), 1b) and 1c) is presented
350 which allows for comparing the effect of considering no inlets and 1 and 2 pairs of inlets per
351 street. The hyetograph (rainfall) and the discharge at the end of the planes, where rainfall-runoff
352 transformation is made, are the same for all the scenarios. The surface outflow is the sum of
353 outflows at the outlets of the street network. As expected, a higher output flow rate is obtained
354 considering no inlets and it diminishes as one includes more inlets. An important observation is
355 that high peak flow attenuation is obtained by routing flow through the street network, i.e. from
356 25 cms (output from all the planes where rainfall-runoff transformation is computed) to only 3.5;
357 2 and 1 cms (output from the entire street network) for no inlets, 1 and 2 pairs of inlets per street,
358 respectively. The legend in Figure 5 represents: Rainfall = hyetograph (intensity times watershed
359 area); Street Network inflow = sum of the discharges at the end of the planes (rainfall-runoff
360 transformation, first module); Intercepted by inlets (1 inlet) = sum of discharges in all the inlets,
361 case with 1 pair of inlets per street; Intercepted by inlets (2 inlets) = same as above, case with 2
362 pairs of inlets per street; Street Network output (No inlets) = sum of discharges at the outlets of
363 the street network case without inlets (or inlets 100% clogged); Street Network output (1 inlet) =
364 same as above considering 1 pair of inlets per street; Street Network output (2 inlets) = same as
365 above considering 2 pairs of inlets per street.

366 A summary of the 5 maximum discharges and corresponding peak times is presented in Table 2
367 for comparison purposes. For instance, node 348 happens to be the one with the largest peak
368 flow for scenarios 1a) and 1b) and the second one for scenario 1c). Regarding the peak flow for
369 node 348, it is reduced to approximately half from no inlets to 1 inlet per street cases and is
370 reduced again to half from 1 inlet to 2 inlets per street cases.
371 In Figure 6, the hydrographs in the 5 nodes with the largest peak flow, i.e. 348, 454, 343, 344
372 and 352, for the scenario 1a) is presented for comparison purposes. All the represented nodes but
373 454 have a single peak whilst 454 have 2 peaks being the second one the largest.
374 In Figure 7, the hydrographs for node 454 in the three scenarios 1x) are presented. It is shown
375 that the double peak is present in all three scenarios although it tends to be smoothed out as the
376 number of inlets per street is increased.
377 A summary of the 5 maximum depths (maximum in the street and in the full simulation time)
378 and corresponding times of occurrence is presented in Table 3. Node 401 is also presented in
379 scenario 1a) for comparison purposes. In the case of scenario 1a) nodes 375, 378 and 633 are
380 those with largest maximum depths which occur almost at the end of the simulation time. In the
381 case of scenario 1b) node 401 is the one with largest maximum depth followed far behind by
382 nodes 488 and 489. In the case of scenario 1c) again node 401 is the one with the largest
383 maximum depth followed far behind by nodes 174, 375, 378 and 633. In light of these results, it
384 can be concluded that in the presence of inlets, the flow redistributes throughout the street
385 network being difficult to predict beforehand the effect of including inlets despite the fact that
386 they are placed uniformly (1 pair by street). Regarding the time of occurrence of the maximum
387 depth, it tends to occur earlier as the number of inlets per street is increased.

388 Figure 8 presents the maximum depth hydrograph for street 401 in the scenarios 1x). As can be
389 observed in this figure, the peak depth does not vary much between the three scenarios but the
390 shape of the falling limb of the depth hydrograph shows significant differences. While the case
391 with no inlets presents a little decrease of the maximum depth towards the ending of the
392 simulation time, the cases with inlets present a large decrease, i.e. 0.6 m for no inlets case versus
393 0.08 and 0.06 m for the case of 1 and 2 inlets per street, respectively. A similar behavior can be
394 observed for street 375, which results are presented in Figure 9. Figure 10 presents the location
395 of streets 174, 375 and 401.
396 In Table 4, the 8 inlets with the maximum flow rate evacuated by inlets are presented for
397 scenarios 1b) and 1c). In general, more flow rate is evacuated when more inlets are present in a
398 given street but in the case of street 401, 2 pairs of inlets evacuate sensibly 2 times more flow
399 rate than 1 pair of inlets. In the other streets only a little more is evacuated with 2 pairs of inlets.
400 The conclusion here is that increasing the number of inlets in some streets could be much more
401 effective than in others.
402 In Figures 11 and 12, the hydrographs of maximum flow rate evacuated by inlets in the 5 streets
403 with the largest values are shown for scenarios 1b) and 1c), respectively. In these figures an
404 oscillating flow rate is detected for street 488 being the amplitude of the oscillation smoother in
405 the case with 2 pairs of inlets per street. This oscillating flow condition is due to the dynamic
406 interaction of flood waves in the street network.
407 Table 5 shows a summary of the total water volume in every model module. In this Table, the
408 first row is the total volume that exits through the planes where rainfall-runoff transformation is
409 performed which is the same that enters to the street network (first module). The second row is
410 the total volume exiting the street network through all outlets (second module). The third row

411 refers to the total outflow volume that exits through the inlets and hence enters to the sewer
412 system (third module). The fourth row shows final volume stored in the street network. The error
413 found (first row minus the sum of the rest of rows) is less than 0.388% for scenario 1a) and
414 0.397% for scenarios 1b) and 1c).
415 If one compares the volume of water intercepted by the inlets in scenarios 1b) and 1c) the
416 conclusion is that the second pair of inlets in the street is much less efficient than the first one.
417 Scenario 2) Considering sewer system (dual drainage)
418 In Figure 13, a summary of hyetograph and main discharges in scenario 2 is presented. In this
419 Figure, the rainfall is considered as in Figure 5; "Street network input" is the sum of the
420 discharges at the end of the planes (rainfall-runoff transformation, first module), "Intercepted by
421 inlets" is the flow rate evacuated by all the inlets; "Street network output" is the flow rate
422 evacuated by all the outlets of the street network and "Sewer system output" is the flow rate
423 exiting from the sewer system (1 single outfall in node 454). By comparing Figure 5 and 13 we
424 can observe the effect of considering the sewer system and its interaction with the flow in the
425 street network (scenarios 1x versus scenario 2). For instance, the maximum flow rate exiting the
426 street network in scenario 2 (i.e. 1.02 cms) remains between the case with 1 pair of inlets per
427 street (1.56 cms) and the one with 2 pairs of inlets per street (0.85 cms). Regarding the maximum
428 flow rate intercepted by inlets, the case in scenario 2 gives a value of 9.83 cms which is
429 somewhat less than that obtained with 1 pair of inlets per street (10.6 cms). The volume
430 intercepted by inlets is also smaller for scenario 2 than scenarios 1b and 1c but the ratios total
431 volume over total number of inlets give 55.2; 38.6 and 21.2 m^3/inlet. It can be concluded that
432 although more inlets mean more volume intercepted, the actual inlet distribution (823 inlets) is
433 more efficient in terms of economical costs than distributing uniformly throughout the street

network (1274 and 2548 inlets for scenarios 1b and 1c, respectively). The effect of the storage of the sewer system is relevant because it permits passing from a peak discharge of 9.83 cms at 2160 s (flow intercepted by inlets) to approximately 5.97 cms at 3680 s (sewer system output) which means a peak flow reduction of 39% as well as a delay of the peak time occurrence of about 25 minutes.

In Figure 14, the hydrographs in the 5 largest outputs of the street network are presented for comparison purposes. In general, they are not too large (maximum of less than 0.18 cms) and different peak discharges and peak times are observed. Flow in node 361 begins to appear almost 30 min later than in node 454 and 372.

Figure 15 represents the total discharge passing from the storm-sewer system to the street network and the number of flooded nodes. At time step 1330 s nodes begin to flood and by time step 3200 s up to 116 nodes are flooded, conveying up to 3.4 cms back to the street network. During approximately one hour at least 40 nodes are flooded (from 2200 to 5900 s) and during approximately 30 minutes at least 80 nodes are flooded (from 2700 to 4400 s).

In Figure 16 the 5 nodes with the largest flooded peak flow are presented. Node 1003 can enter to the street network a maximum discharge of more than 0.6 cms and remains above 0.4 cms for approximately 15 minutes.

Instabilities in Figures 15 and 16 appear because of the coupling time used. When the hydraulic grade line in a given node is very close the ground elevation but above it, that node become flooded and this situation will remain at least until the next calling of SWMM5 is produced. Meanwhile, water has been passing from the sewer system towards the streets and the hydraulic grade line could decrease below the ground elevation so that in the next calling of SWMM5 that

node is not flooded anymore. This situation being repeated over and over generates such instabilities.

Analysis considering different hazard criteria. Dual drainage case

Four hazard criteria were used to detect critical points: maximum depth of 0.30 m, maximum velocity of 1 m/s, maximum product of depth times velocity of 0.5 m^2/s and maximum product depth times velocity squared of 1.23 m^3/s^2. Figures 17 to 20 show the time series for the four parameters used to assess the hazard of the street runoff in the 5 streets where the values are the largest. Such time series can be used to observe if either of these limits is exceeded and for how long this situation lasts.

For the system used as an example, it can be concluded that criteria of stability to tilt ($y*V$) and stability to slipping ($y*V^2$) are never exceeded whilst criterion of maximum velocity is exceeded only in street 514 for less than 10 minutes. This behavior is as expected due to the small slopes of the street network in the Village of Dolton.

According to the hazard criteria defined above the more restrictive criterion is that of depth which gives 49 streets with depths greater than 0.30 m for as long as 200 minutes. Table 6 gives a list of those streets. Streets 375, 378 and 633 show depths as high as 0.75 m and it is apparent that water remains stagnant till the end of the study so a potential measure to improve the situation could be to place more inlets in a suitable position. In streets 375 and 378 no sewer systems exists so it could be advisable to design a sewer system for this area. Figure 21 shows an example of how the results could be displayed. This way of showing results can help detect quickly areas where node flooding is frequent but not a hazard regarding the maximum water depth. The opposite, this is, water depth greater than 0.30 m for a long time and no flooded nodes could indicate the areas where more inlets are needed and would also be more efficient. Streets

479 with water depth greater than 0.30 m and flooded nodes hardly could improve the situation
480 adding more inlets because the existing inlets could be the responsible for that situation.
481
482 **Conclusions**
483 The present work describes the application of a model for simulating dual drainage in urban
484 areas. This model consists of four modules which simulates (1) rainfall-runoff transformation,
485 (2) one-dimensional flow routing on a street network, (3) flow evacuation by the inlets located in
486 the streets and (4) flow interaction between surface water on the streets and underground storm-
487 water system by interfacing with the SWMM5 engine. The rainfall-runoff transformation (first
488 module) uses the kinematic wave approximation for the overland flow routing and the Green-
489 Ampt method for simulating the infiltration process. The street flow routing (second module) is
490 based on a finite-volume shock-capturing scheme that solves the full conservative Saint-Venant
491 equations and can be used to simulate subcritical and supercritical flows. The inlet interception
492 module (third module) is based on the HEC-22 equations. The underground storm-water flows
493 (fourth module) are modeled using SWMM5.
494 The main contributions are: the use of a rainfall-runoff transformation module which
495 incorporates the flow generated directly to the street network; the use of empirical relationships
496 by Nanía et al (2004, 2011) to determine the flow distribution in four-branch junctions of the
497 street network which have supercritical and subcritical flows; the simulation of flow evacuated
498 by inlets through the implementation of the HEC-22 formulation; and the flow interaction
499 between surface water on the streets and underground storm-water by interfacing the street
500 network model with the SWMM5 engine.

In order to illustrate the potential of the proposed model, it was applied to an urban catchment in the Village of Dolton, which is a southern suburb of the metropolitan area of Chicago. Four scenarios were implemented: 1a) street network with no inlets, i.e. representing inlets 100% clogged; 1b) street network with one pair of inlets per street; 1c) street network with two pairs of inlets per street; and 2) street network with actual inlets and sewer system. Cases of scenarios 1x) are examples of use of the model to decide number, location and type of inlets. Complete model can be used either to (1) verify the capacity of an actual sewer system and study the consequences of changes in an actual sewer system or (2) design a new sewer system.

In any scenario it is possible to apply different criteria to assess the runoff hazard. A summary of hazard criteria is presented and four criteria were adapted to be applied to the catchment of Dolton. In this case, the application of those criteria concluded that only the criterion of high depths (greater than 0.30 m) was exceeded in 49 out of 637 streets for as long as 200 minutes. Some of the critical points correspond to zones with no sewer system. No problems were found regarding to the criterion of high velocity flows and the criteria which include the velocity as parameter given the relatively flat topography.

Overall, the proposed model is shown to be a suitable tool for identification of critical zones of urban flooding (e.g., zones with high water depths and flow velocities) that could be useful to undertake appropriate measures for drainage control (e.g., to increase number or size of inlets), to determine the consequences of different degrees of inlet clogging, and to assess the flooding hazard through the application of any suitable hazard criteria.

Acknowledgements

523 The partial funding from the Metropolitan Water Reclamation District of Greater Chicago's
524 Tunnel and Reservoir Plan (TARP) Project for a two-month stay of the first author in the
525 University of Illinois at Urbana-Champaign is acknowledged. The results and conclusions
526 presented above are solely those of the authors and do not represent the opinion of any agency.
527

528 **References**

529 Abt, S.R.; Wittler, R.J.; Taylor, A. (1989) *Predicting Human Instability in Flood Flows*.
530 Proceedings of the 1989 National Conference on Hydraulic Engineering, ASCE, New York, pp.
531 70-76.

532 Aronica, G.T. and L.G. Lanza (2005) Drainage efficiency in urban areas: a case study.
533 Hydrological Proccesses, Vol 19, 1105-1119.

534 Bazin, P.-H.; H. Nakagawa; K. Kawaike; A. Paquier; E. Mignot (2013) Modelling flow
535 exchanges between a street and an underground drainage pipe during urban floods. Novatech
536 2013.

537 Cantone, J. and A.R. Schmidt (2011). Improved understanding and prediction of the hydrologic
538 response of highly urbanized catchments through development of the Illinois Urban Hydrologic
539 Model. Water Resources Research, Vol. 48, Issue 8, DOI: 10.1029/2010WR009330.

540 Chen A.S.; S. Djordjevic; J. Leandro and D.A. Savic (2010) An analysis of the combined
541 consequences of pluvial and fluvial flooding. Water Science and Technology, Vol. 62, No. 7, pp.
542 1491-1498.

543 Chow, V.T.; Maidment, D.R.; Mays, L.W. (1988) *Applied Hydrology*. McGraw-Hill, New York.

544 Chow, V.T. and Yen, B.C. (1976) "Urban Stormwater Runoff: Determination of Volumes and
545 Flowrates", *Environmental Protection Technology Series*, EPA-600/2-76-116, US

City of Austin Dept. of Public Works (1977). *Drainage Criteria Manual*, First Edition, Austin, Texas.

Clark County Regional Flood Control District (1999*) Hydrologic Criteria and Drainage Design Manual*. Available on: http://www.co.clark.nv.us, Clark City, NV.

Chaudhry, M. H. (1987). *Applied hydraulic transients*, Van Nostrand Reinhold, New York.

EPA Municipal Environmental Research Laboratory, Cincinnati, Ohio.

Djordjevic, S.; D. Prodanovic and C. Maksimovic (1999) An approach to simulation of dual drainage. Water Science and Technology, Vol. 39, No. 9, pp. 95-103.

Djordjevic, S.; D. Prodanovic; C. Maksimovic; M. Ivetic and D. Savic (2005) SIPSON – Simulation of Interaction between Pipe flow and Surface Overland flow in Networks. Water Science and technology, Vol. 52, No. 5, pp. 275-283.

Djordjevic, S.; A.J. Saul, G.R. Tabor; J. Blanksby; I. Galambos; N. Sabtu; and G. Sailor (2013) Experimental and numerical investigation of interactions between above and below ground drainage systems. Water Science and technology, Vol. 67, No. 3, pp. 535-542.

Federal Highway Administration (2001) *Urban Drainage Design Manual*. Hydraulic Engineering Circular Nº 22 (HEC-22), second edition. U.S. Department of Transportation.

Hsu M.H.; S.H. Chen; T.J. Chang (2000) Inundation simulation for urban drainage basin with storm sewer. Journal of Hydrology, Vol. 234, pp. 21-37.

Kumar Dey, A. and Seiji Kamioka (2007) An integrated modeling approach to predict flooding on urban basin. Water Science and Technology, Vol. 55, No. 4, pp. 19-29.

Leon, A.S. (2007) Improved Modeling of Unsteady Free Surface, Pressurized and Mixed Flows in Storm-sewer Systems, Ph.D. thesis, University of Illinois at Urbana-Champaign.

568 Leon, A.S.; Ghidaoui, M.S.; Schmidt, A.R.; and García, M.H. (2006). Godunov-type solutions
569 for transient flows in sewers. J. Hydraul. Engng., 132(8), 800-813.
570 León, A. S.; Ghidaoui, M. S.; Schmidt, A. R.; and Garcia, M. H. (2009) "Application of
571 Godunov-type schemes to transient mixed flows." *Journal of Hydraulic Research*, 47(2), 147-
572 156.
573 Leon, A. S.; Ghidaoui, M. S.; Schmidt, A. R.; and Garcia, M. H. (2010a) "A robust two-equation
574 model for transient-mixed flows." Journal of Hydraulic Research, 48(1), 44-56.
575 Leon, A. S.; Liu, X.; Ghidaoui, M. S.; Schmidt, A. R.; and Garcia, M. H. (2010b) "Junction and
576 drop-shaft boundary conditions for modeling free-surface, pressurized, and mixed free-surface
577 pressurized transient flows." Journal of Hydraulic Engineering, 136(10), 705-715.
578 Leon, A. S.; Gifford-Miears, C. H.; and Choi, Y. (2013) "Well-Balanced Scheme for Modeling
579 Open-Channel and Surcharged Flows in Steep-Slope Closed Conduit Systems." Journal of
580 Hydraulic Engineering, 139(4), 374-384.
581 MWRDGC (2013) *Tunnel and Reservoir Plan*, http://www.mwrd.org/irj/portal/anonymous/tarp,
582 accessed on July 2014.
583 Martins, R; J. Leandro; R.F. Carvalho (2014) Characterization of the hydraulic performance of a
584 gully under drainage conditions. Water Science and Technology, in Press.
585 Nania-Escobar, L.S. (1999) *Numerical and experimental methodology for danger analysis of*
586 *urban runoff in a street network*. PhD Thesis. E.T.S.I.C.C.P., Universitat Politècnica de
587 Catalunya. Barcelona, Spain, ISBN: 978-84-690-5623-3 (In spanish).
588 Nanía, L.; M. Gómez; and J. Dolz (2007) *Surface stormwater hazard assessment in steep urban*
589 *areas. Case of the city of Mendoza, Argentina*. Urban Water Journal, Vol. 4, Nº2, pp. 119-130,
590 ISSN: 1573-062X.

591 Nanía-Escobar, L.S.; M. Gómez-Valentín; J. Dolz-Ripollés (2006) *Análisis de la peligrosidad de*
592 *la escorrentía pluvial en zona urbana utilizando un enfoque numérico-experimental*. Revista
593 Ingeniería Hidráulica en México, Vol. XXI, Nro. 2. pp. 5-15, Morelos, México. ISSN: 0186-
594 4076.
595 Nanía, L.; M. Gómez; and J. Dolz (2004) *Experimental Study of the Dividing Flow in Steep*
596 *Street Crossings*. Journal of Hydraulic Research. Vol. 42, Nº 4, pp. 406-412.
597 Nanía, L.; M. Gómez; J. Dolz; P.Comas; and J. Pomares (2011) *Experimental Study of*
598 *Subcritical Dividing Flow in an Equal-Width, Four-Branch Junction*. Journal of Hydraulic
599 Engineering, ASCE, Vol. 137, Nº10, pp. 1298-1305.
600 New South Wales Government (2005) *Flood Development Manual*, Sydney.
601 Schmitt, T.G; M. Thomas; N. Ettrich. (2004) Analysis and Modeling of flooding in urban
602 drainage systems. Journal of Hydrology, Vol. 299, pp. 300-311.
603 Sección de Ingeniería Hidráulica e Hidrológica, UPC (2001) *Definición de Criterios de Riesgo*
604 *para el Flujo en Calles. Análisis del espaciamiento para rejas e imbornales utilizados en la*
605 *Ciudad de Barcelona*. E.T.S.E.C.C.P., Universitat Politècnica de Catalunya, Barcelona, Spain (In
606 Spanish).
607 Témez P., J.R. (1992) "Control del desarrollo urbano en las zonas inundables". In: *Inundaciones*
608 *y redes de drenaje urbano*, J.Dolz, M.Gómez, J.P.Martín (ed.), Monografías del Colegio de
609 Ingenieros de Caminos, Canales y Puertos No. 10, Madrid, pp.105-115 (in Spanish).
610 Wright-McLaughlin (1969) *Urban storm drainage criteria manual*. Urban Drainage and Flood
611 Control District, Denver, CO.

Table 1: Main watershed characteristics.

Characteristic	Pervious area	Impervious area
Percentage of total area	42.6	57.4
Average slope	0.0133	0.0133
Manning coefficient	0.2	0.015
Depression storage [mm]	12.7	1.27
Hydraulic conductivity [mm/h]	10.7	
Effective saturation	0.418	
Effective porosity	0.412	
Suction head [m]	0.169	

Table 2: Top 5 nodes with maximum surface outflow discharge and peak time for scenarios 1x).

Scenario 1a) No Inlets			**Scenario 1b) 1 Inlet**			**Scenario 1c) 2 Inlets**		
Node	**Q_{max}**	**T_p**	**Node**	**Q_{max}**	**T_p**	**Node**	**Q_{max}**	**T_p**
	cms	s		cms	s		cms	s
348	0.737	3800	348	0.351	4000	454	0.19	2500
454	0.654	4900	454	0.277	3300	348	0.188	3700
343	0.637	4500	343	0.229	4100	343	0.096	3800
344	0.498	4700	344	0.158	4700	372	0.073	2500
352	0.215	3400	372	0.11	3400	361	0.062	3400

Table 3: Top 5 nodes with maximum depth and time of occurrence for scenarios 1x).

Scenario 1a) No Inlets			**Scenario 1b) 1 Inlet**			**Scenario 1c) 2 Inlets**		
Street	$\mathbf{y_{max}}$	$\mathbf{T_p}$	**Street**	$\mathbf{y_{max}}$	$\mathbf{T_p}$	**Street**	$\mathbf{y_{max}}$	$\mathbf{T_p}$
	m	s		m	s		m	s
375	1.02	10200	401	0.7	2800	401	0.68	2600
378	1.02	10200	488	0.48	5200	174	0.43	3900
633	1.02	10200	489	0.48	5200	375	0.4	3300
328	0.89	10200	483	0.47	5000	378	0.4	3300
338	0.89	10200	174	0.47	4100	633	0.4	3300
401*	0.73	3200						

Note: *Not in the Top5

Table 4: Top 8 streets with maximum flow rate evacuated by inlets and time of occurrence for scenarios 1b) and 1c).

Scenario 1b) 1 inlet per street			**Scenario 1c) 2 inlets per street**		
Street	**Q_{max}**	**T_p**	**Street**	**Q_{max}**	**T_p**
	cms	s		cms	s
401	0.223	2300	401	0.45	2600
488	0.199	3800	488	0.225	3500
487	0.147	4600	487	0.184	3800
378	0.126	3000	406	0.128	3500
79	0.126	3900	413	0.120	3000
486	0.120	4400	190	0.120	2800
633	0.107	3200	307	0.111	3200
190	0.096	3100	438	0.108	2800

Table 5: Global mass balance in cubic meters per seconds (cms) for scenarios 1x) and 2).

Item	Scenario 1a) No Inlets	Scenario 1b) 1 pair of inlets per str.	Scenario 1c) 2 pairs of inlets per str.	Scenario 2) Real inlets
Vol. entering street network	59459	59459	59459	59459
Vol. exiting street network	17554	5613	2673	3615
Vol. intercepted by inlets	0	49183	53980	45393
Final storage in street network	42136	4899	3042	10656
Error (%)	0.388	0.397	0.397	0.345

Table 6: List of streets with water depths greater than 0.30 m and duration.

Street	Minutes with depth > 0.30m	Street	Minutes with depth > 0.30m
63	75	375	205
65	110	378	205
67	200	401	205
73	75	407	25
74	70	408	15
76	100	412	30
77	110	413	25
78	200	414	30
79	200	415	25
114	40	420	80
162	45	421	110
164	105	437	85
165	185	438	105
166	185	482	15
167	185	483	195
170	55	486	5
190	45	487	100
194	185	488	195
196	180	489	195
198	185	490	85
202	180	616	100
207	180	617	90
213	185	621	45
220	50	633	205
221	50		

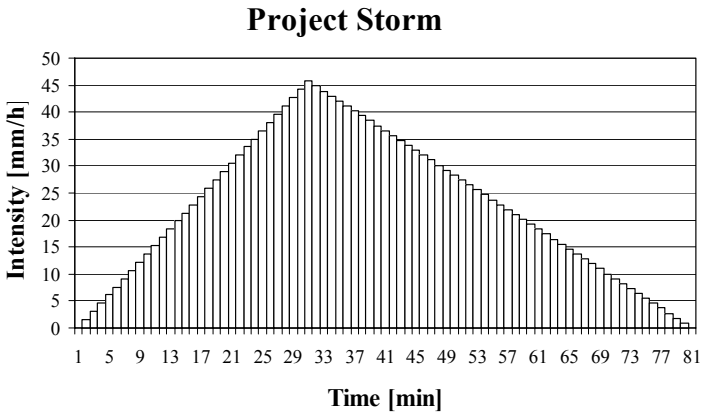

Figure 1**:** Simplified rainfall hyetograph for Chicago city on July 2nd, 1960 (Adapted from Chow and Yen, 1976).

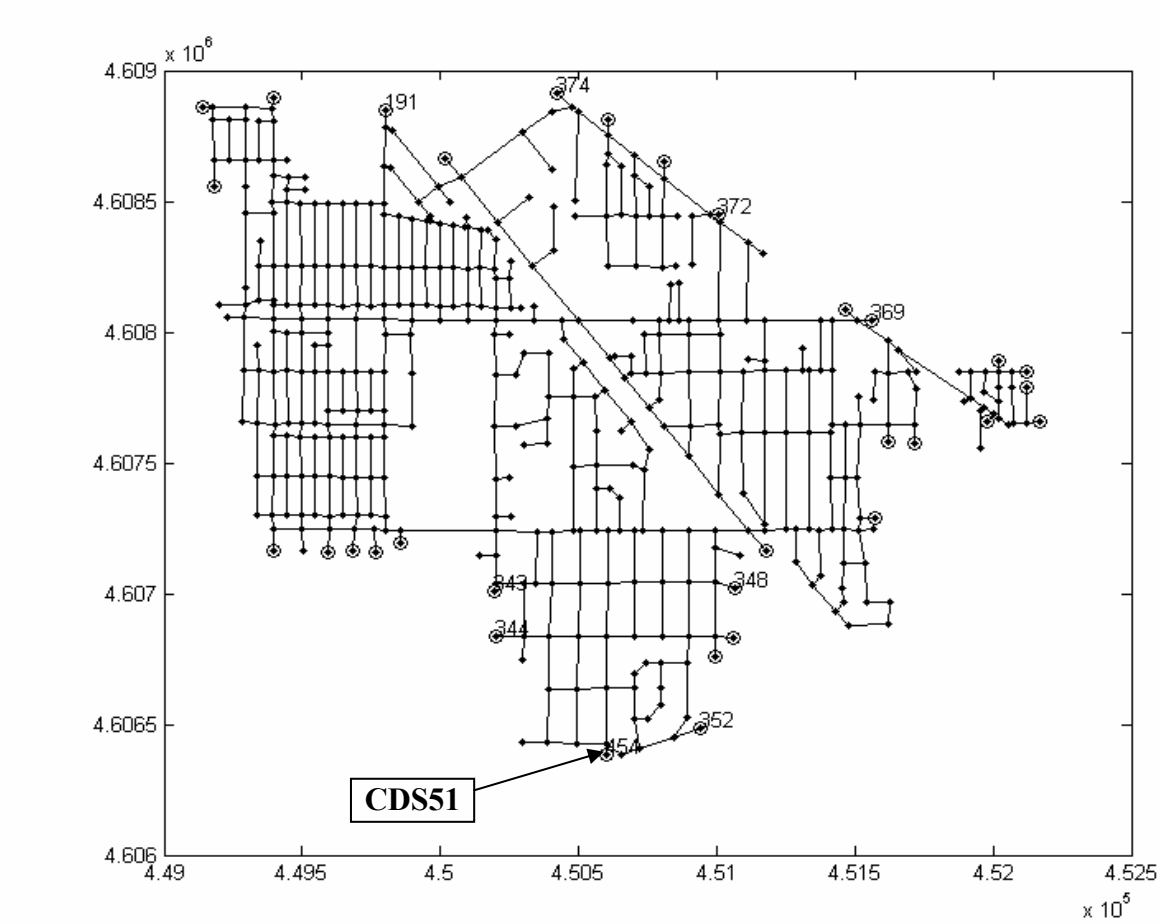

Figure 2: Street network showing as circles the nodes with outflow discharges and with numbers inclusive the ones with the largest discharges. CDS51 dropshaft coincides with node 454 (Distance in meters).

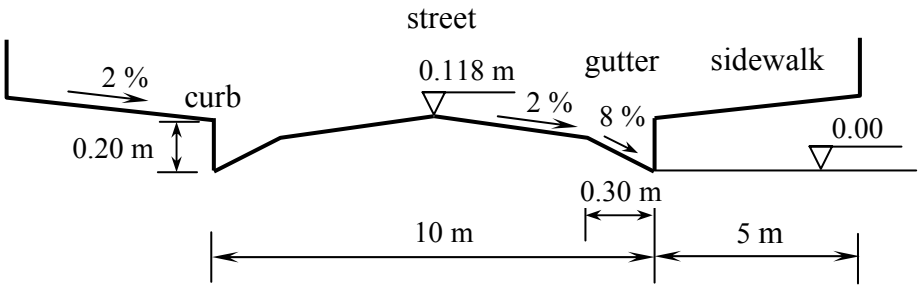

Figure 3: Modeled street cross-section (not to scale).

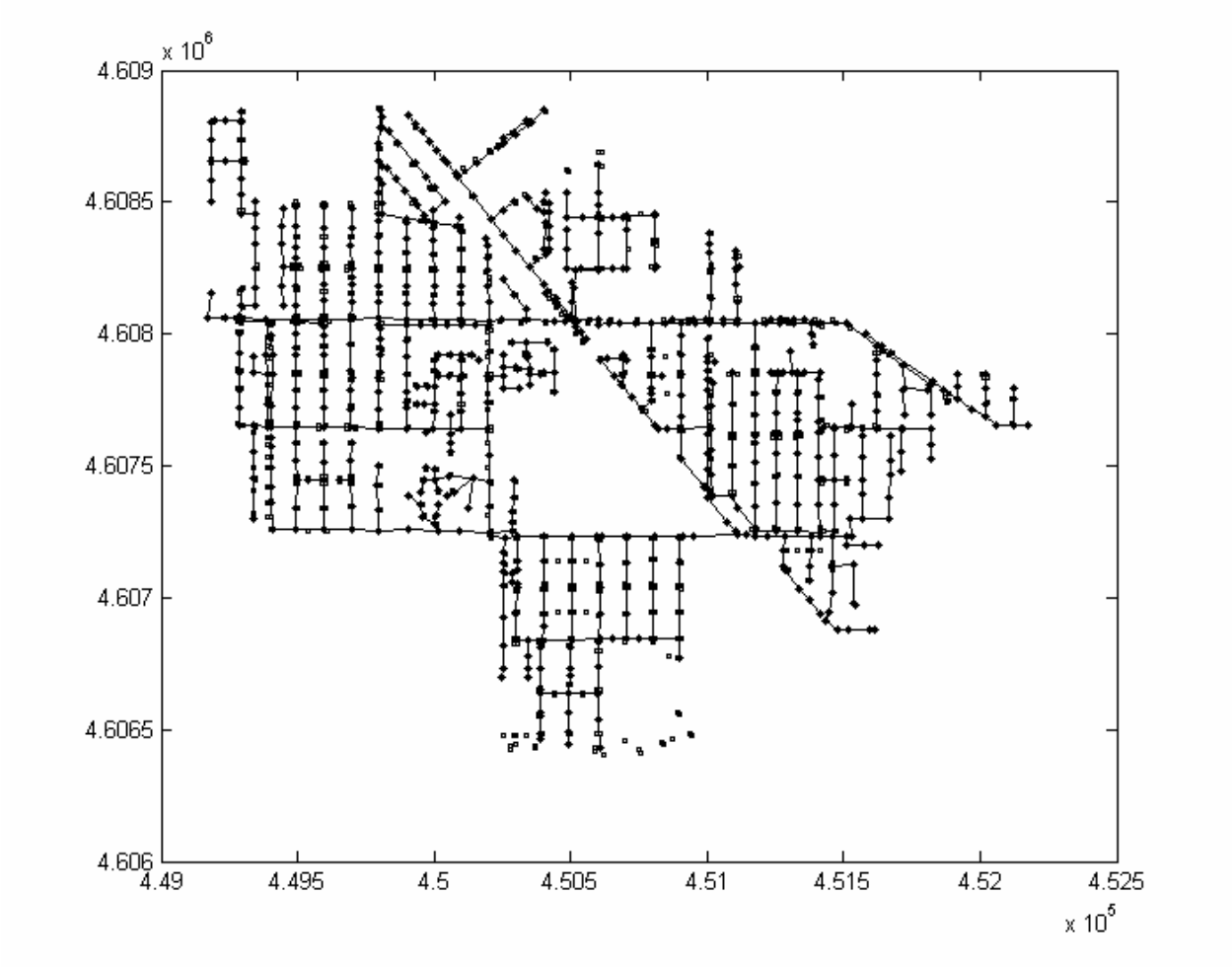

Figure 4: Sewer network showing nodes as circles and inlets as squares (Distance in meters).

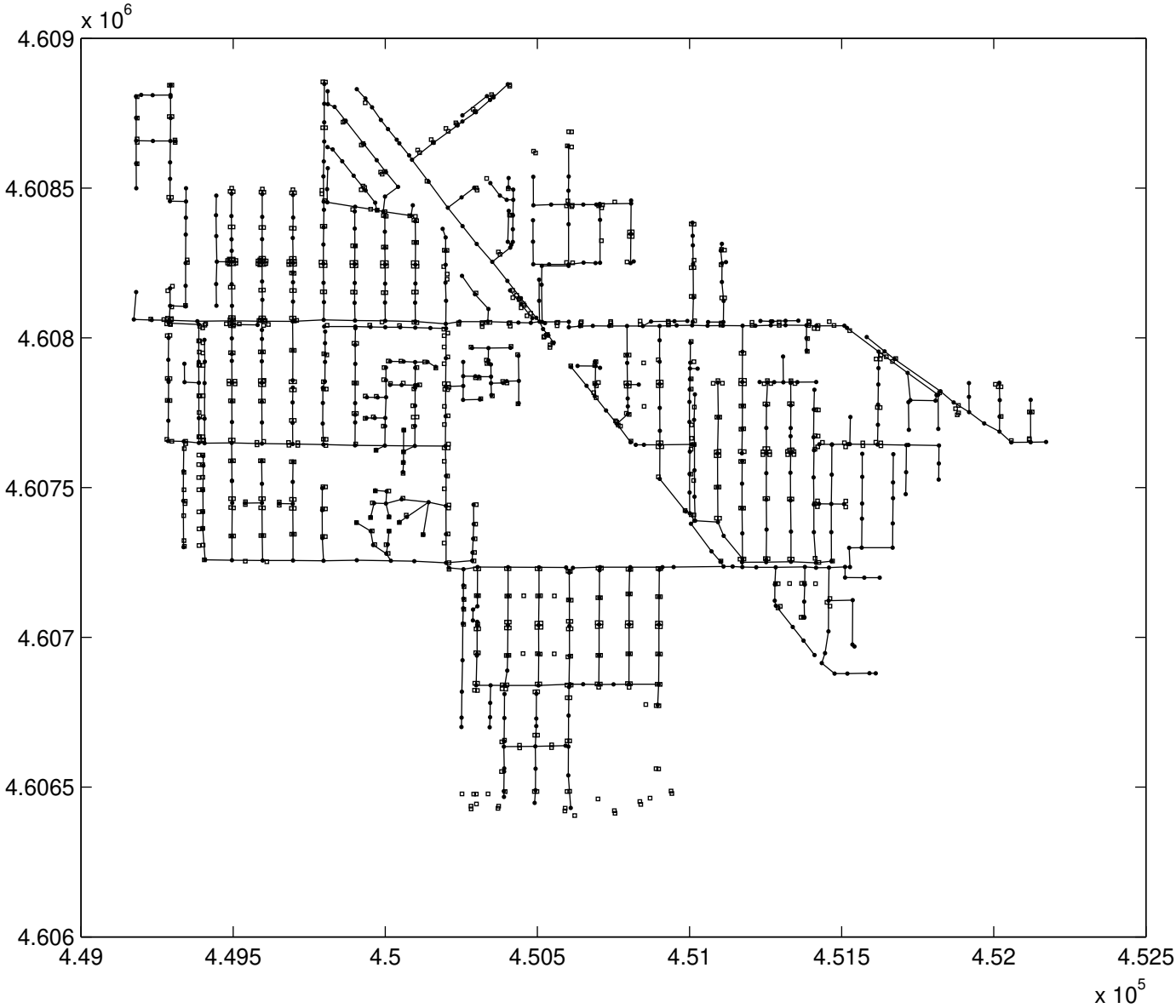
x 10^6
4.609
4.6085
4.608
4.6075
4.607
4.6065
4.606
4.49
4.495
4.5
4.505
4.51
4.515
4.52
4.525
x 10^5

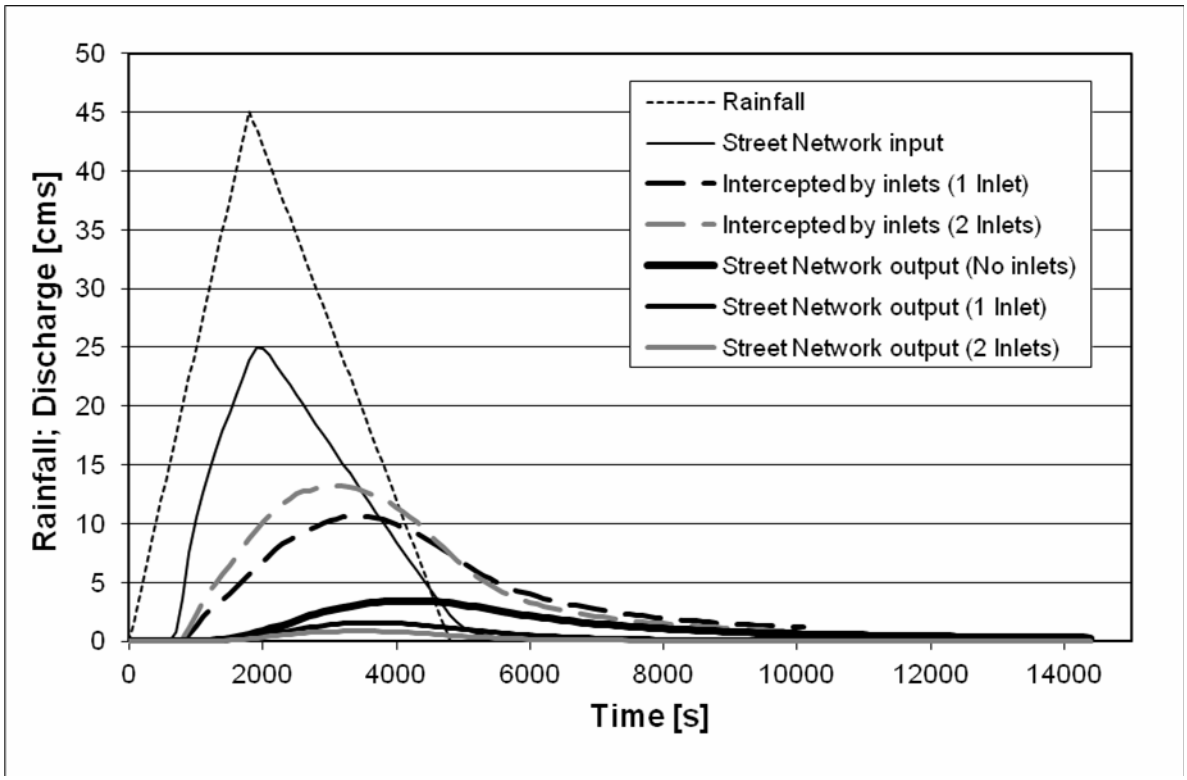

Figure 5: Summary of hyetograph and main discharges in scenarios 1a), 1b) and 1c).

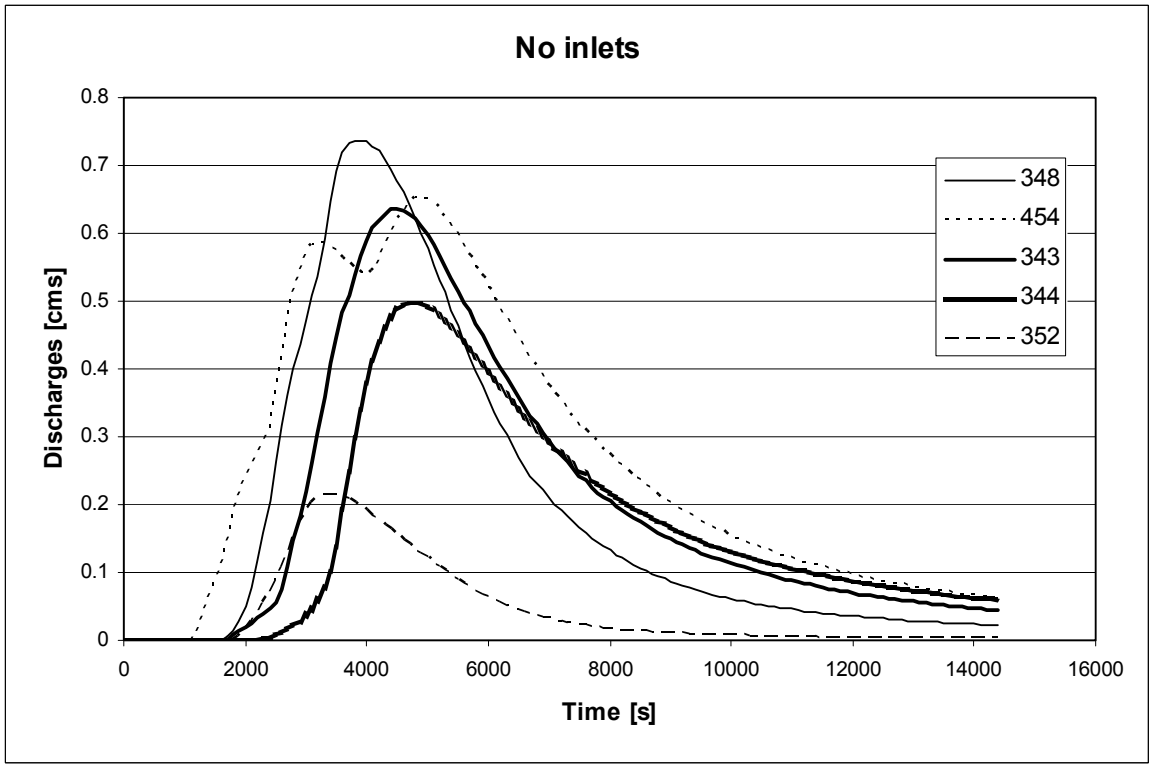

Figure 6: Hydrographs in the 5 nodes with the largest peak flow, i.e. 348, 454, 343, 344 and 352, for the scenario 1a) = no inlets.

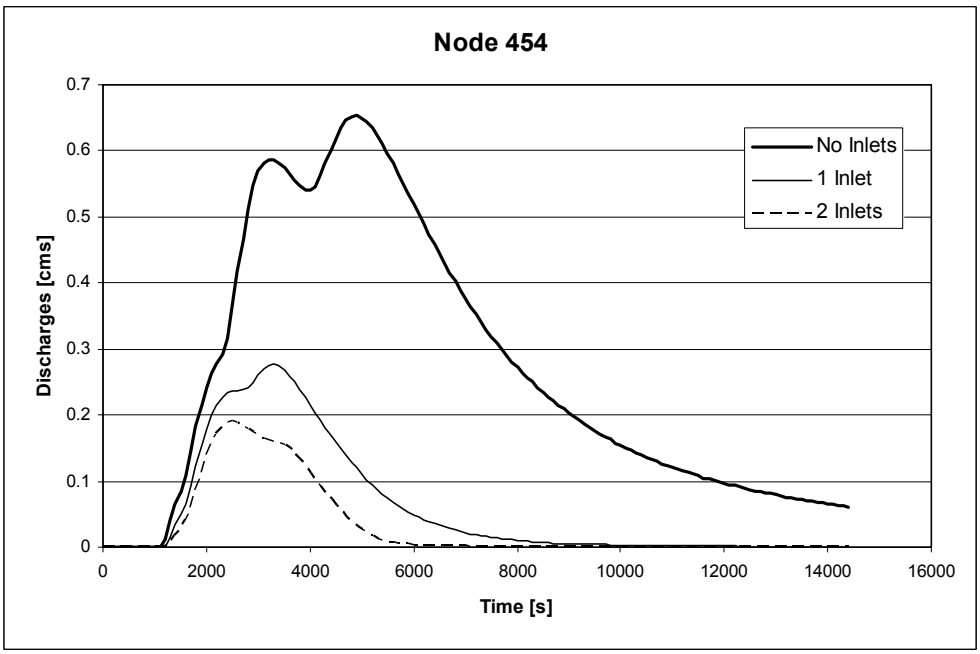

Figure 7: Hydrographs in the node 454 for scenarios 1a) no inlets; 1b)1 pair of inlets per street; and 1c) 2 pairs of inlets per street.

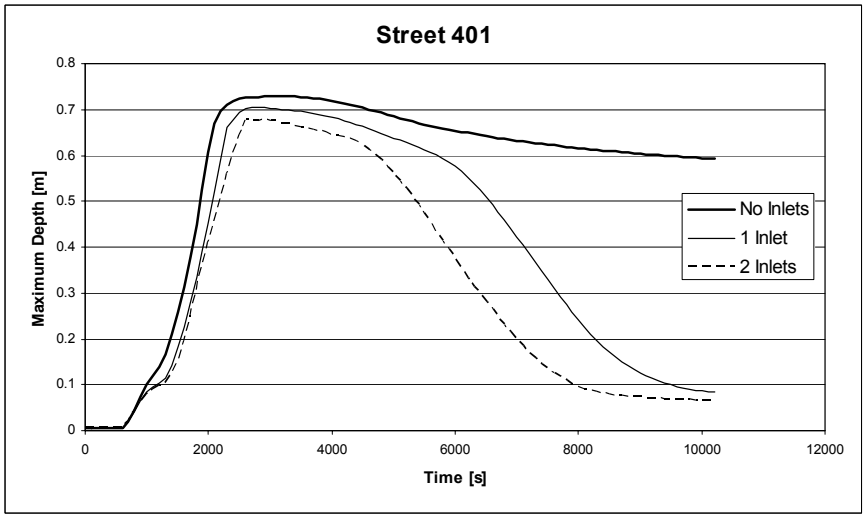

Figure 8: Maximum depth hydrographs in the node 401 for scenarios 1a) no inlets; 1b) 1 pair of inlets per street; and 1c) 2 pairs of inlets per street.

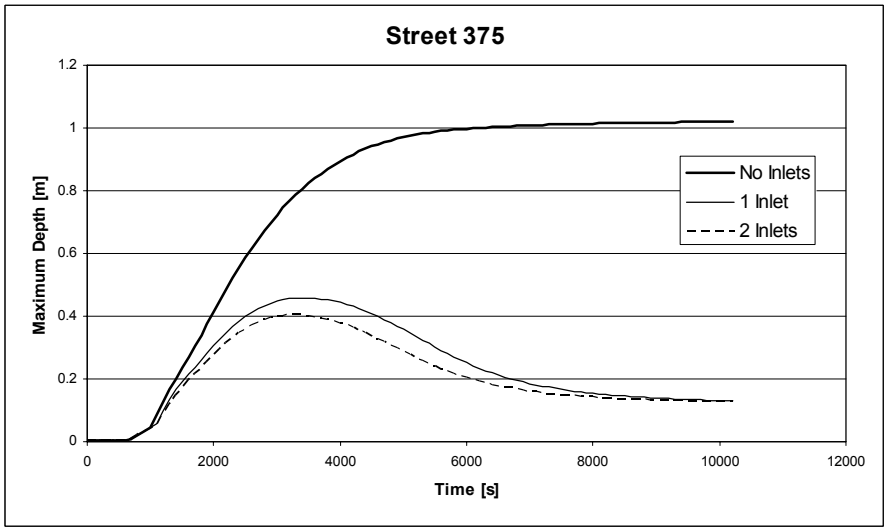

Figure 9: Maximum depth hydrographs in the node 375 for scenarios 1a) no inlets; 1b) 1 pair of inlets per street; and 1c) 2 pairs of inlets per street.

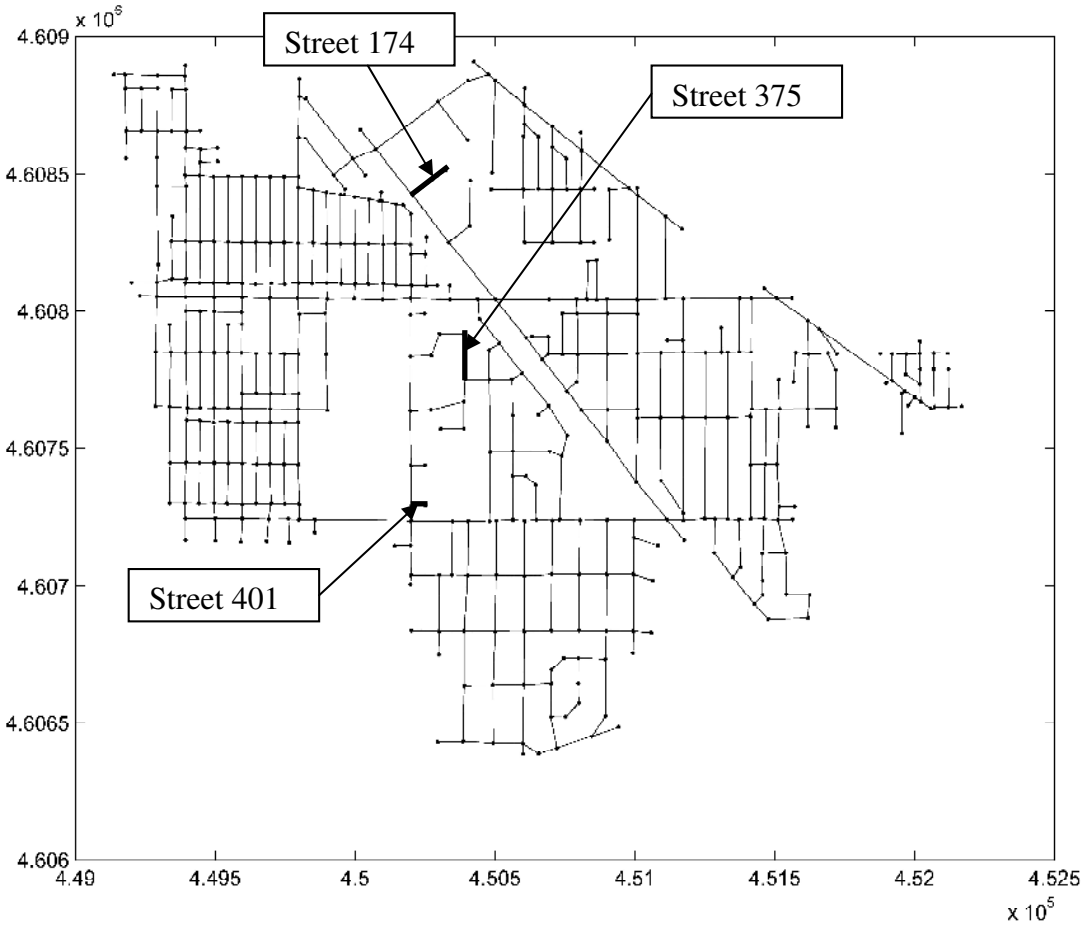

Figure 10: Location of streets 174, 375 and 401 in the street network.

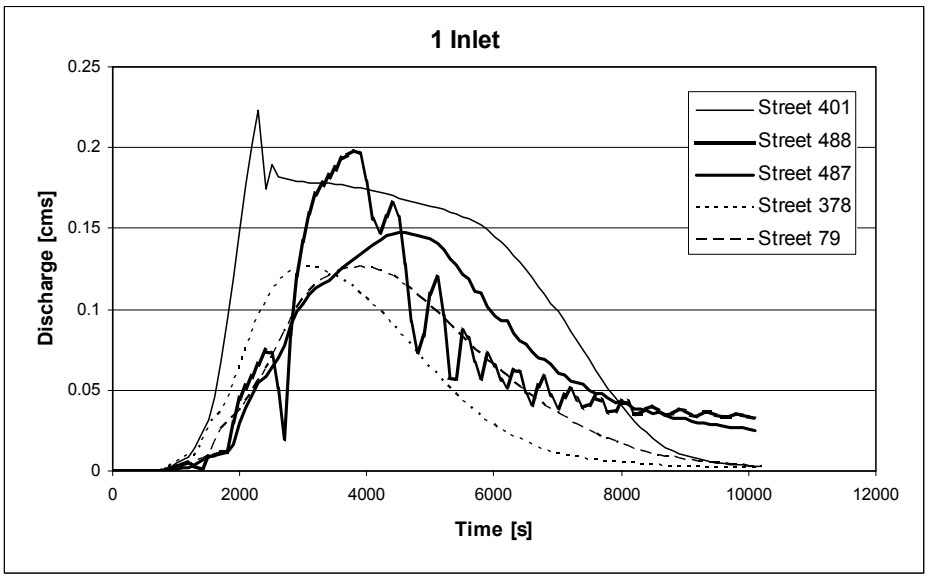

Figure 11: Hydrographs of maximum flow rate evacuated by inlets in streets 401, 488, 487, 378 and 79, in case of scenario 1b) 1 pair of inlets per street.

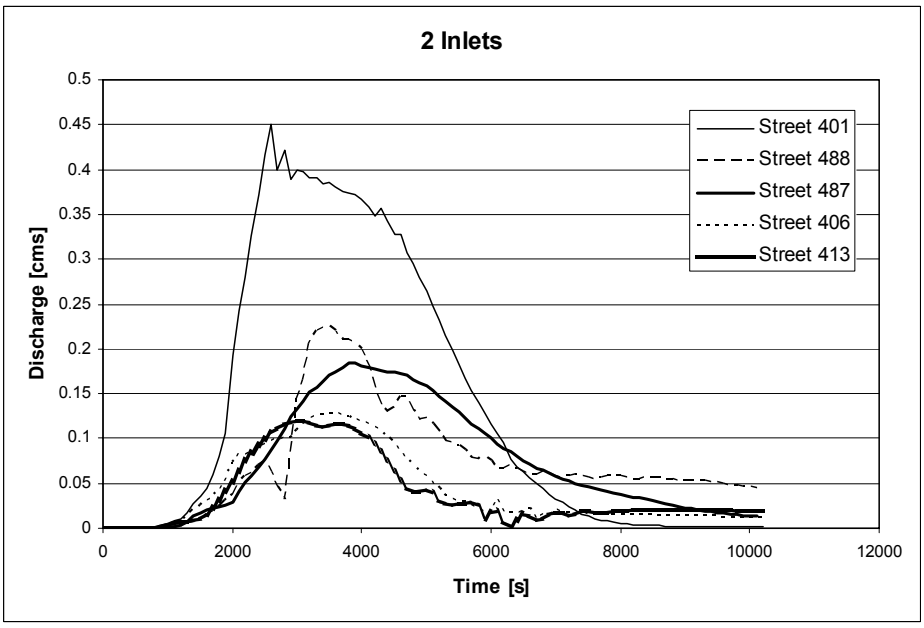

Figure 12: Hydrographs of maximum flow rate evacuated by inlets in streets 401, 488, 487, 406 and 413, in case of scenario 1c) 2 pairs of inlets per street.

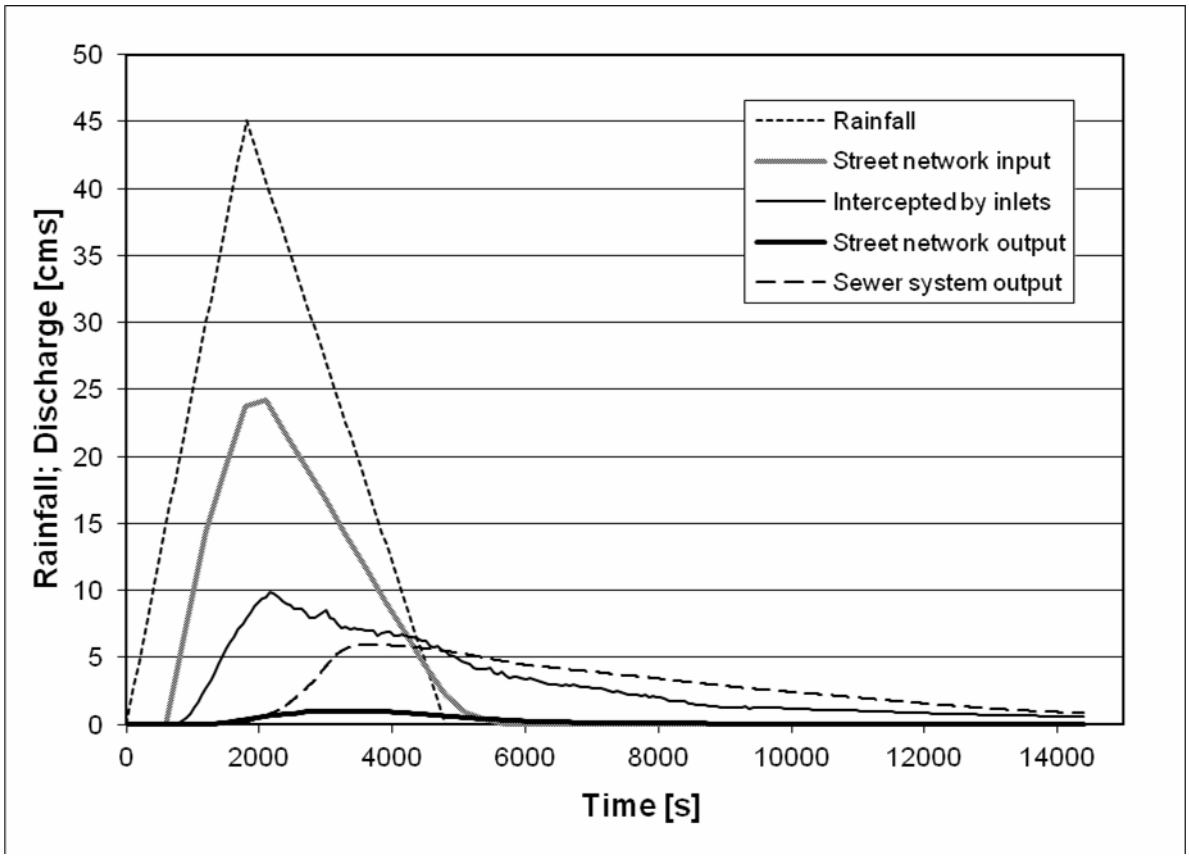

Figure 13: Summary of hyetograph and main discharges in scenarios 2.

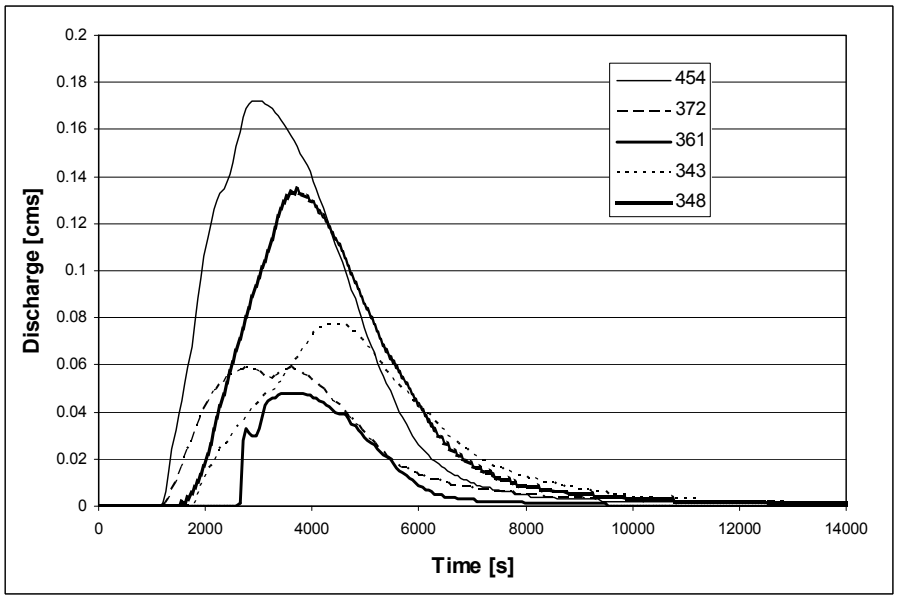

Figure 14: Hydrographs in the 5 nodes with the largest peak flow in the outputs of the street network, i.e. 454, 372, 361, 343 and 348, for scenario 2) dual drainage.

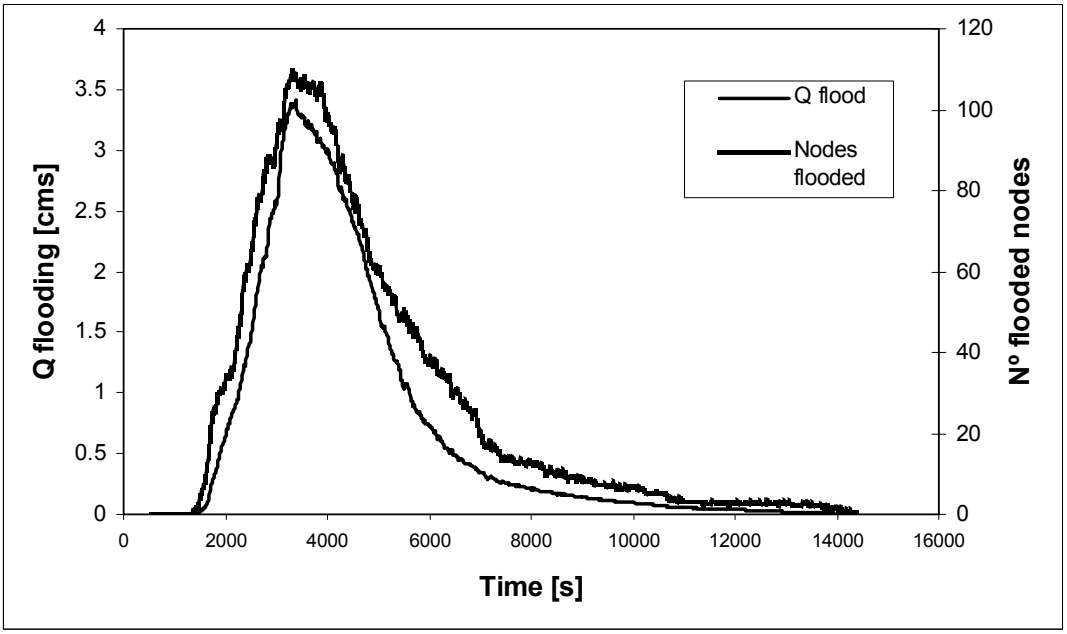

Figure 15: Time series of discharge passing from the storm-sewer system to the street network and number of flooded nodes.

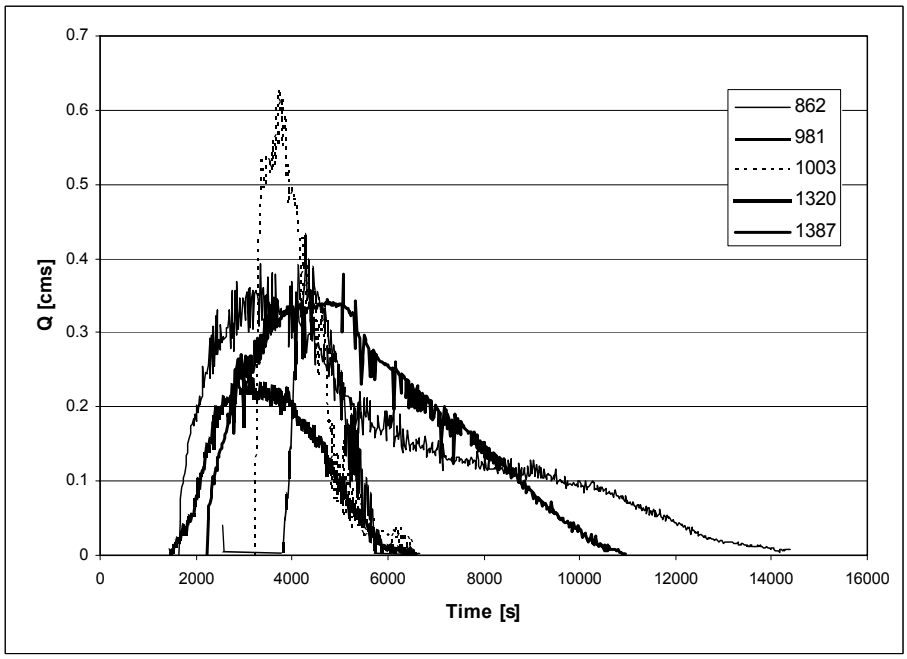

Figure 16: Hydrographs in the 5 nodes with the largest flooded peak flow, i.e. 862, 981, 1003, 1320 and 1387, for scenario 2) dual drainage.

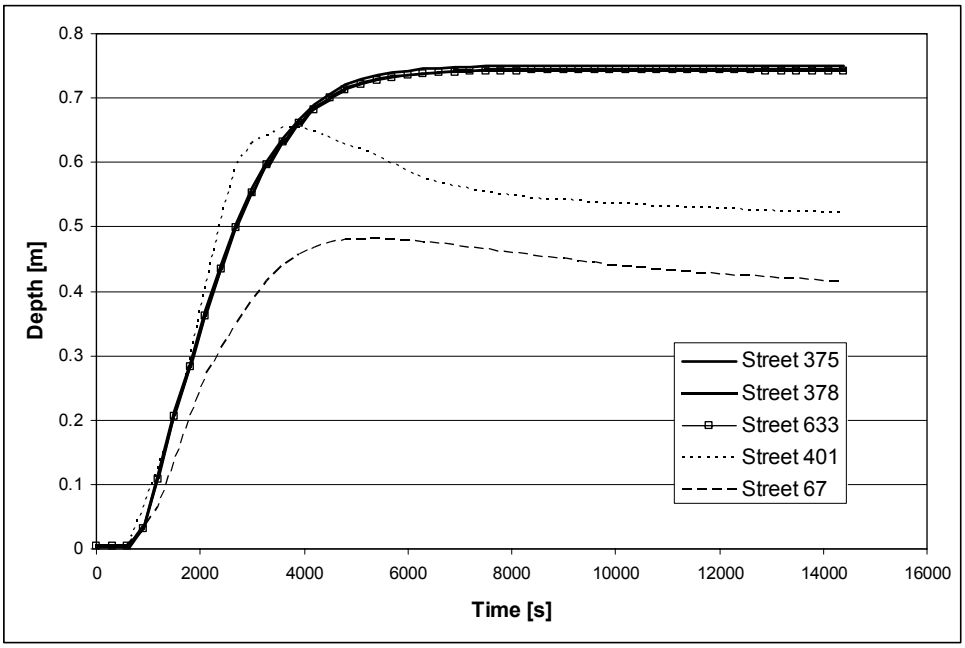

Figure 17: Evolution of maximum depth over time in the 5 streets with the largest depths. Scenario 2).

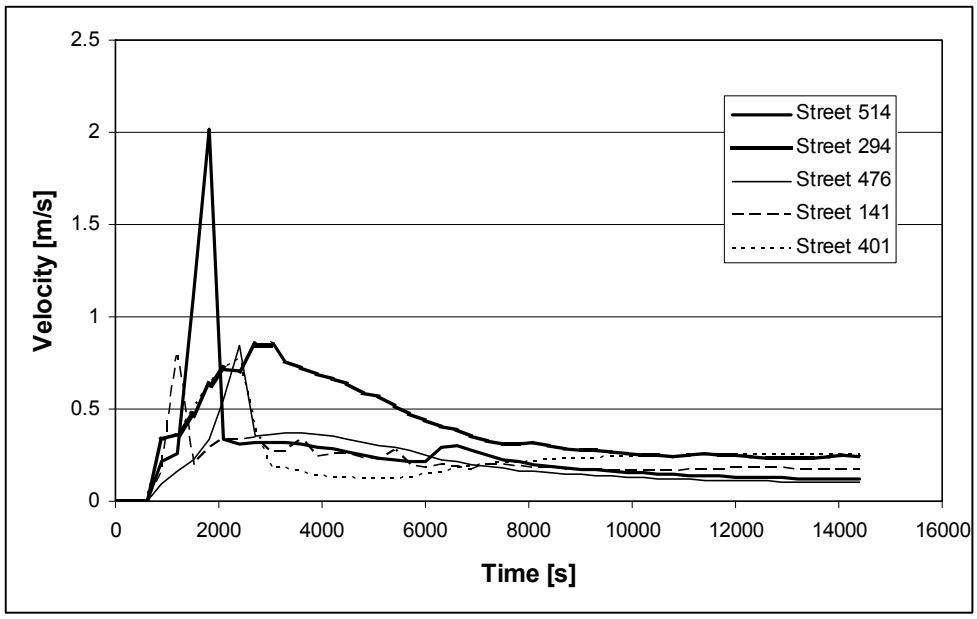

Figure 18: Evolution of maximum velocity over time in the 5 streets with the largest velocities. Scenario 2.

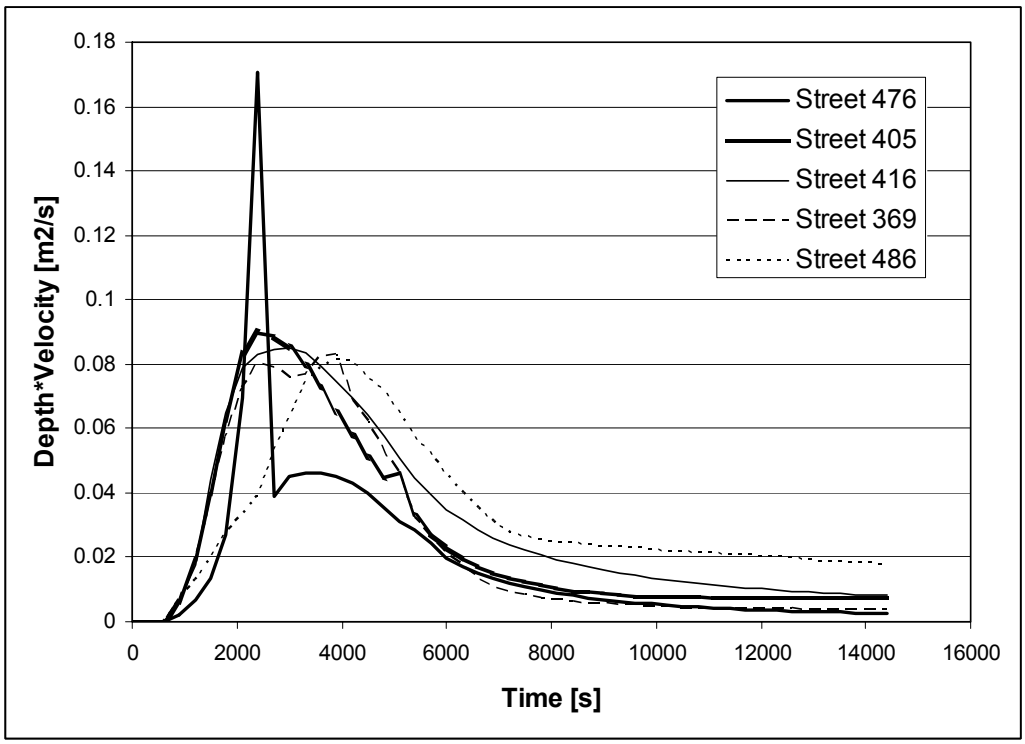

Figure 19: Evolution of maximum product of depth times velocity over time in the 5 streets with the largest values. Scenario 2.

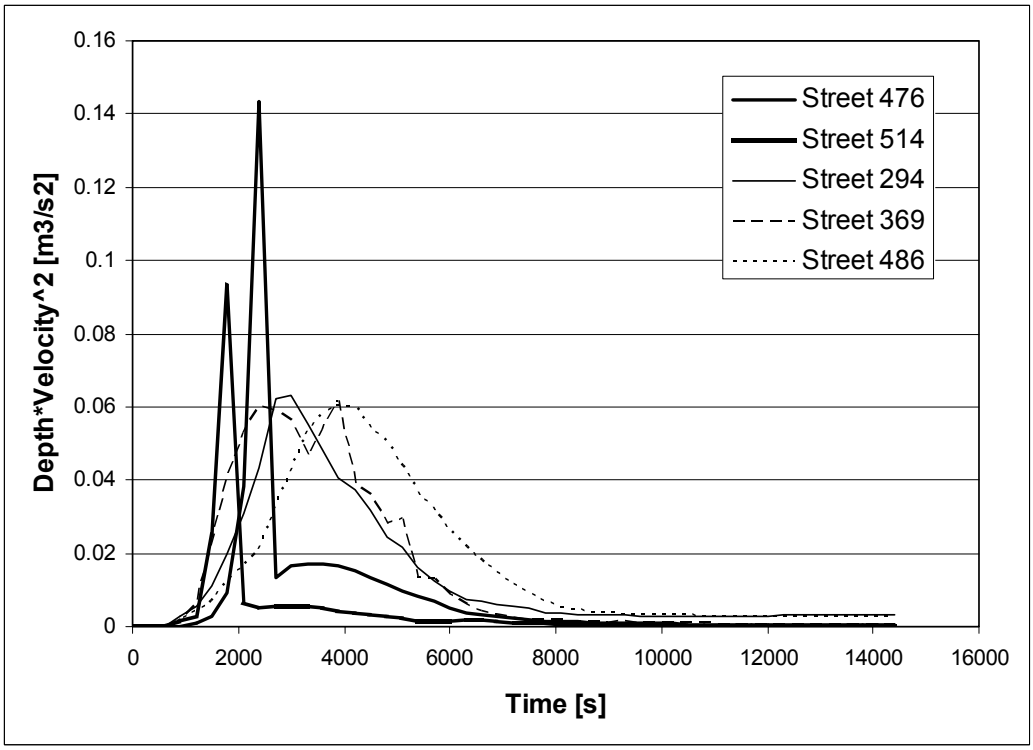

Figure 20: Evolution of maximum product of depth times velocity squared over time in the 5 streets with the largest values. Scenario 2).

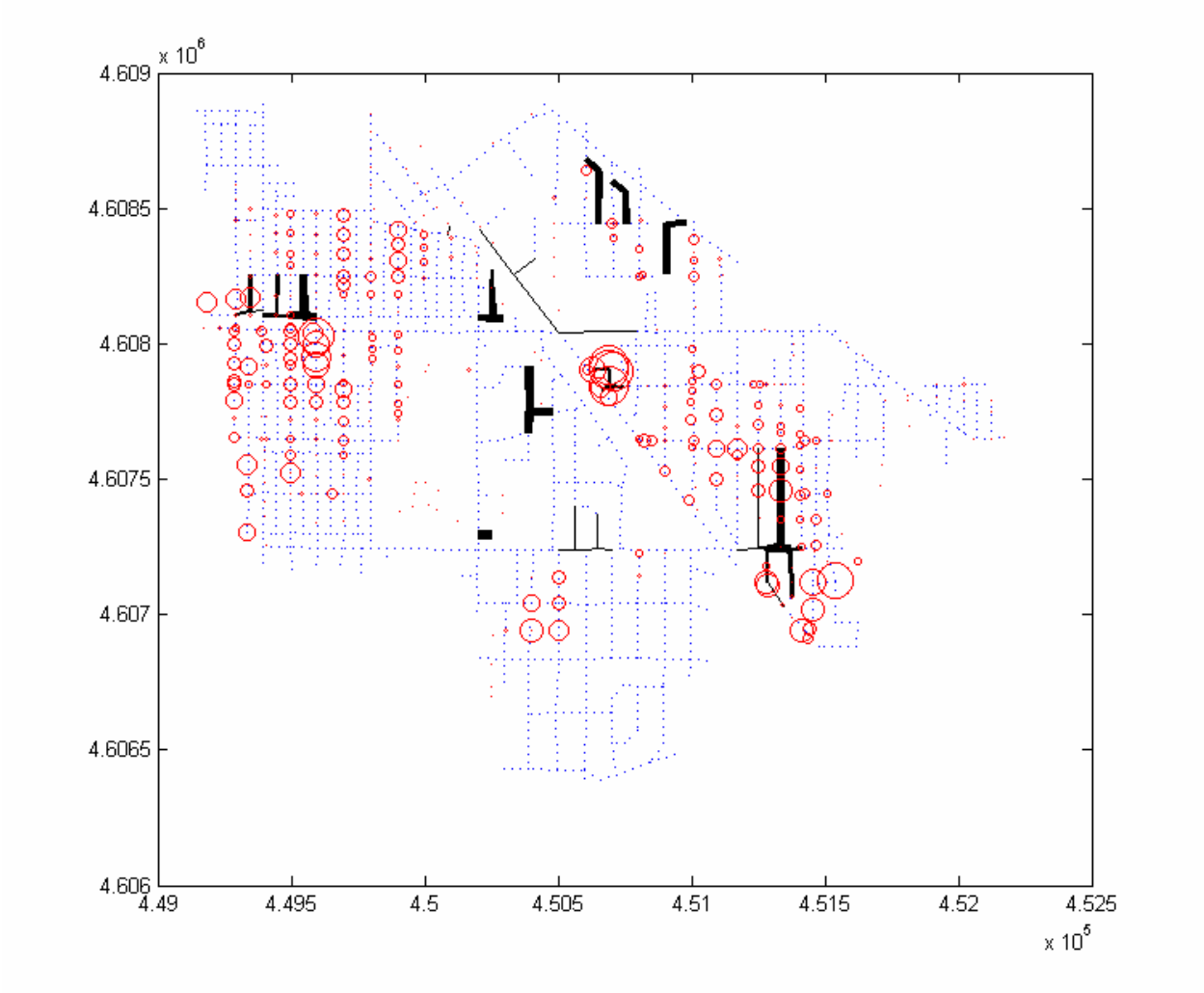

Figure 21: Map showing a summary of results. Dotted lines = street network; circles = flooded sewer nodes (diameters related to duration); lines = streets with maximum water depths greater than 0.30 m (thickness related to duration).

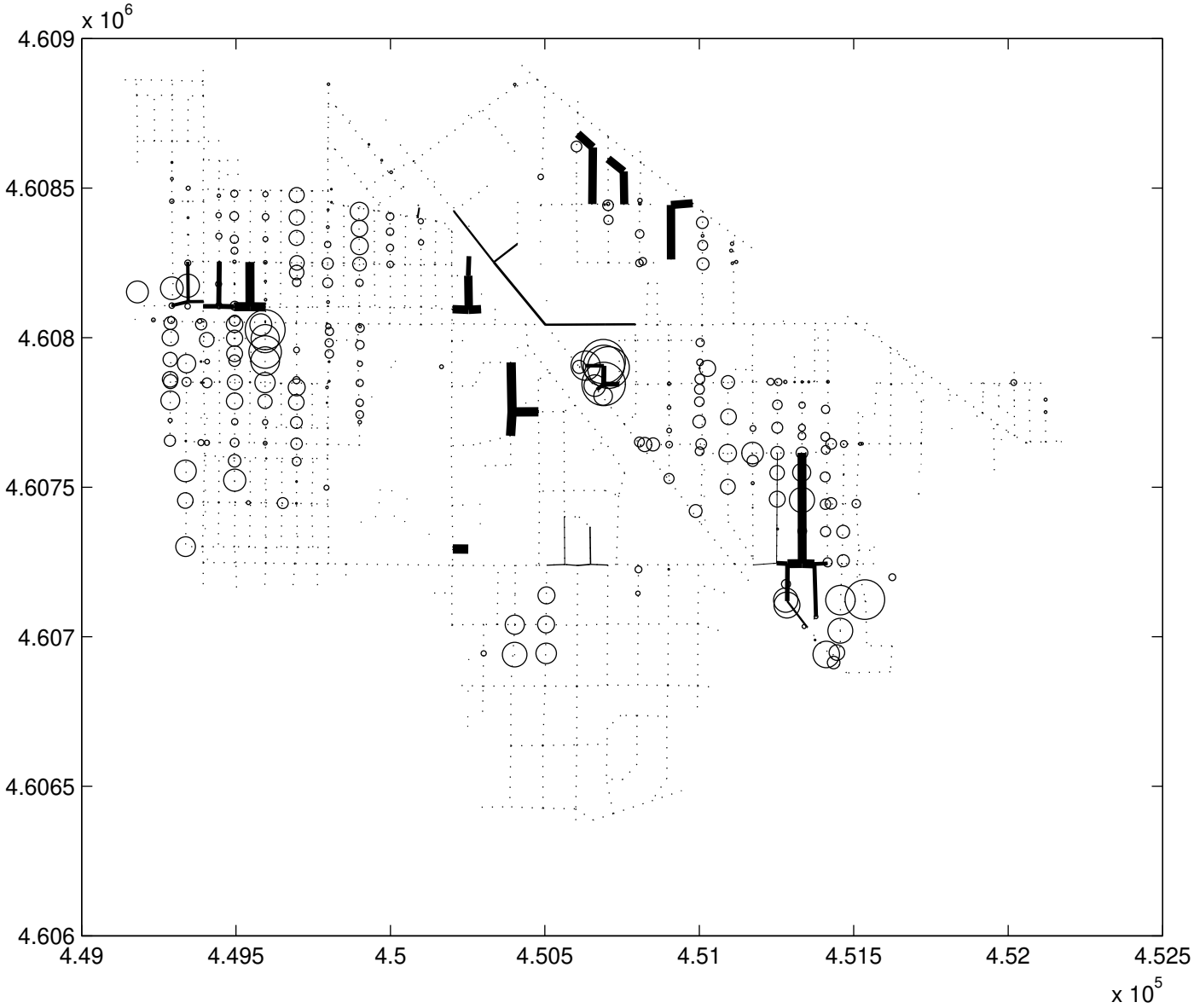
x 10^6
4.609
4.6085
4.608
4.6075
4.607
4.6065
4.606
4.49
4.495
4.5
4.505
4.51
4.515
4.52
4.525
x 10^5